DOI: 10.1111/geb.12747

RESEARCH PAPER

WILEY Global Ecology and Biogeography A Journal of Macroecology

Global importance of large-diameter trees

James A. Lutz[1*] | Tucker J. Furniss[1*] | Daniel J. Johnson[2] | Stuart J. Davies[3,4] | David Allen[5] | Alfonso Alonso[6] | Kristina J. Anderson-Teixeira[3,7] | Ana Andrade[8] | Jennifer Baltzer[9] | Kendall M. L. Becker[1] | Erika M. Blomdahl[1] | Norman A. Bourg[7,10] | Sarayudh Bunyavejchewin[11] | David F. R. P. Burslem[12] | C. Alina Cansler[13] | Ke Cao[14] | Min Cao[15] | Dairon Cárdenas[16] | Li-Wan Chang[17] | Kuo-Jung Chao[18] | Wei-Chun Chao[19] | Jyh-Min Chiang[20] | Chengjin Chu[21] | George B. Chuyong[22] | Keith Clay[23] | Richard Condit[24,25] | Susan Cordell[26] | Handanakere S. Dattaraja[27] | Alvaro Duque[28] | Corneille E. N. Ewango[29] | Gunter A. Fischer[30] | Christine Fletcher[31] | James A. Freund[13] | Christian Giardina[26] | Sara J. Germain[1] | Gregory S. Gilbert[32] | Zhanqing Hao[33] | Terese Hart[34] | Billy C. H. Hau[35] | Fangliang He[36] | Andrew Hector[37] | Robert W. Howe[38] | Chang-Fu Hsieh[39] | Yue-Hua Hu[14] | Stephen P. Hubbell[40] | Faith M. Inman-Narahari[26] | Akira Itoh[41] | David Janík[42] | Abdul Rahman Kassim[31] | David Kenfack[3,4] | Lisa Korte[6] | Kamil Král[42] | Andrew J. Larson[43] | YiDe Li[44] | Yiching Lin[45] | Shirong Liu[46] | Shawn Lum[47] | Keping Ma[14] | Jean-Remy Makana[29] | Yadvinder Malhi[48] | Sean M. McMahon[49] | William J. McShea[7] | Hervé R. Memiaghe[50] | Xiangcheng Mi[14] | Michael Morecroft[48] | Paul M. Musili[51] | Jonathan A. Myers[52] | Vojtech Novotny[53,54] | Alexandre de Oliveira[55] | Perry Ong[56] | David A. Orwig[57] | Rebecca Ostertag[58] | Geoffrey G. Parker[59] | Rajit Patankar[60] | Richard P. Phillips[23] | Glen Reynolds[61] | Lawren Sack[40] | Guo-Zhang M. Song[62] | Sheng-Hsin Su[17] | Raman Sukumar[63] | I-Fang Sun[64] | Hebbalalu S. Suresh[27] | Mark E. Swanson[65] | Sylvester Tan[66] | Duncan W. Thomas[67] | Jill Thompson[68] | Maria Uriarte[69] | Renato Valencia[70] | Alberto Vicentini[55] | Tomáš Vrška[42] | Xugao Wang[33] | George D. Weiblen[71] | Amy Wolf[38] | Shu-Hui Wu[72,73] | Han Xu[44] | Takuo Yamakura[41] | Sandra Yap[56] | Jess K. Zimmerman[74]

*Authors contributed equally.

[1]Wildland Resources Department, Utah State University, Logan, Utah

[2]Biology Department, Utah State University, Logan, Utah

[3]Center for Tropical Forest Science-Forest Global Earth Observatory, Smithsonian Tropical Research Institute, Panama, Republic of Panama

[4]Department of Botany, National Museum of Natural History, Washington, DC

[5]Department of Biology, Middlebury College, Middlebury, Vermont

[6]Center for Conservation and Sustainability, Smithsonian Conservation Biology Institute, National Zoological Park, Washington, DC

[7]Conservation Ecology Center, Smithsonian Conservation Biology Institute, National Zoological Park, Washington, DC

[8]Projeto Dinâmica Biológica de Fragmentos Florestais, Instituto Nacional de Pesquisas da Amazônia - INPA, Petrópolis, Manaus, Amazonas, Brazil

[9]Biology Department, Wilfrid Laurier University, Waterloo, Ontario, Canada

[10]U.S. Geological Survey, Hydrological-Ecological Interactions Branch, Water Mission Area, Reston, Virginia

[11]Royal Thai Forest Department, Kasetsart and Mahidol Universities, Bangkok, Thailand

[12]School of Biological Sciences, University of Aberdeen, Aberdeen, United Kingdom

[13]School of Environmental and Forest Science, University of Washington, Seattle, Washington

[14]State Key Laboratory of Vegetation and Environmental Change, Institute of Botany, Chinese Academy of Sciences, Xiangshan, Beijing

[15]Key Laboratory of Tropical Forest Ecology, Xishuangbanna Tropical Botanical Garden, Chinese Academy of Sciences, Mengla, Yunnan

[16]Instituto Amazónico de Investiagciones Científicas Sinchi, Bogotá, D.C., Colombia

[17]Taiwan Forestry Research Institute, Taipei

[18]International Master Program of Agriculture, National Chung Hsing University, Taichung

[19]Department of Forestry and Natural Resources, National Chiayi University, Chiayi City

[20]Department of Life Science, Tunghai University, Taichung

[21]Department of Ecology and Evolution, Sun Yat-sen University, Guangzhou

[22]Department of Botany and Plant Physiology, University of Buea, Buea, Cameroon

[23]Department of Biology, Indiana University, Bloomington, Indiana

[24]Field Museum of Natural History, Chicago, Illinois

[25]Morton Arboretum, Lisle, Illinois

[26]Institute of Pacific Islands Forestry, USDA Forest Service, Hilo, Hawaii

[27]Centre for Ecological Sciences, Indian Institute of Science, Bangalore, Karnataka, India

[28]Departamento de Ciencias Forestales, Universidad Nacional de Colombia Sede Medellín, Medellín, Colombia

[29]Centre de Formation et de Recherche en Conservation Forestière, Gombe, Democratic Republic of Congo

[30]Kadoorie Farm & Botanic Garden Corporation, Hong Kong

[31]Forest Environmental Division, Forest Research Institute of Malaysia, Kepong, Malaysia

[32]Environmental Studies Department, University of California, Santa Cruz, Santa Cruz, California

[33]Key Laboratory of Forest Ecology and Management, Institute of Applied Ecology, Chinese Academy of Sciences, Shenyang

[34]Wildlife Conservation Society, Ituri, Democratic Republic of Congo

[35]School of Biological Sciences, University of Hong Kong, Hong Kong

[36]Department of Renewable Resources, University of Alberta, Edmonton, Alberta, Canada

[37]Plant Sciences, University of Oxford, Oxford, United Kingdom

[38]Department of Natural and Applied Sciences, University of Wisconsin-Green Bay, Green Bay, Wisconsin

[39]Institute of Ecology and Evolutionary Biology, National Taiwan University, Taipei

[40]Department of Ecology and Evolutionary Biology, University of California, Los Angeles, Los Angeles, California

[41]Graduate School of Science, Osaka City University, Osaka, Japan

[42]Department of Forest Ecology, Silva Tarouca Research Institute, Brno, Czech Republic

[43]Department of Forest Management, W.A. Franke College of Forestry and Conservation, University of Montana, Missoula, Montana

[44]Research Institute of Tropical Forestry, Chinese Academy of Forestry, Guangzhou

[45]Life Science Department, Tunghai University, Taichung

[46]Institute of Forest Ecology, Environment and Protection, Chinese Academy of Forestry, Beijing

[47]Asian School of the Environment, Nanyang Technological University, Singapore, Singapore

[48]School of Geography and the Environment, Oxford University, Oxford, United Kingdom

[49]Center for Tropical Forest Science-Forest Global Earth Observatory, Forest Ecology Group, Smithsonian Environmental Research Center, Edgewater, Maryland

[50]Institut de Recherche en Ecologie Tropicale, Centre National de la Recherche Scientifique et Technologique, Libreville, Gabon

[51]East African Herbarium, Botany Department, National Museum of Kenya, Nairobi, Kenya

[52]Department of Biology & Tyson Research Center, Washington University in St. Louis, St. Louis, Missouri

[53]New Guinea Binatang Research Centre, Madang, Papua New Guinea

[54]Biology Centre, Academy of Sciences of the Czech Republic and Faculty of Science, University of South Bohemia, Ceske Budejovice, Czech Republic

[55]Department of Ecology, University of São Paulo, São Paulo, Brazil

[56]Institute of Arts and Sciences, Far Eastern University Manila, Manila, Philippines

[57]Harvard Forest, Harvard University, Petersham, Massachusetts

[58]Department of Biology, University of Hawaii, Hilo, Hawaii

[59]Forest Ecology Group, Smithsonian Environmental Research Center, Edgewater, Maryland

[60]National Ecological Observatory Network (NEON) Inc., Denton, Texas

[61]The Royal Society SEARRP (UK/Malaysia), Danum Valley, Malaysia

[62]Department of Soil and Water Conservation, National Chung Hsing University, Taichung

[63]Centre for Ecological Sciences and Divecha Centre for Climate Change, Indian Institute of Science, Bangalore, Karnataka, India

[64]Department of Natural Resources and Environmental Studies, National Dong Hwa University, Hualian

[65]School of the Environment, Washington State University, Pullman, Washington

[66]Sarawak Forest Department, Kuching, Sarawak, Malaysia

[67]School of Biological Sciences, Washington State University, Vancouver, Washington

[68]Center for Ecology and Hydrology, Bush Estate, Penicuik Midlothian, Edinburgh, United Kingdom

[69]Department of Ecology, Evolution, and Environmental Biology, Columbia University, New York, New York

[70]School of Biological Sciences, Pontificia Universidad Católica del Ecuador, Quito, Ecuador

[71]Department of Plant & Microbial Biology, University of Minnesota, St. Paul, Minnesota

[72]Taiwan Forestry Research Institute, Council of Agriculture, Taipei

[73]Department of Biological Sciences, National Sun Yat-sen University, Kaohsiung

[74]Department of Environmental Sciences, University of Puerto Rico, Rio Piedras, Puerto Rico

Correspondence
James A. Lutz, Wildland Resources Department, Utah State University, 5230 Old Main Hill, Logan, UT 84322.
Email: james.lutz@usu.edu

Funding information
Utah Agricultural Experiment Station, Grant/Award Number: 1153; National Natural Science Foundation of China; National Science Foundation, Grant/Award Number: 1354741 and 1545761

Editor: Andrew Kerkhoff

Abstract

Aim: To examine the contribution of large-diameter trees to biomass, stand structure, and species richness across forest biomes.

Location: Global.

Time period: Early 21st century.

Major taxa studied: Woody plants.

Methods: We examined the contribution of large trees to forest density, richness and biomass using a global network of 48 large (from 2 to 60 ha) forest plots representing 5,601,473 stems across 9,298 species and 210 plant families. This contribution was assessed using three metrics: the largest 1% of trees $\geq$ 1 cm diameter at breast height (DBH), all trees $\geq$ 60 cm DBH, and those rank-ordered largest trees that cumulatively comprise 50% of forest biomass.

Results: Averaged across these 48 forest plots, the largest 1% of trees $\geq$ 1 cm DBH comprised 50% of aboveground live biomass, with hectare-scale standard deviation of 26%. Trees $\geq$ 60 cm DBH comprised 41% of aboveground live tree biomass. The size of the largest trees correlated with total forest biomass ($r^2 = .62$, $p < .001$). Large-diameter trees in high biomass forests represented far fewer species relative to overall forest richness ($r^2 = .45$, $p < .001$). Forests with more diverse large-diameter tree communities were comprised of smaller trees ($r^2 = .33$, $p < .001$). Lower large-diameter richness was associated with large-diameter trees being individuals of more common species ($r^2 = .17$, $p = .002$). The concentration of biomass in the largest 1% of trees declined with increasing absolute latitude ($r^2 = .46$, $p < .001$), as did forest density ($r^2 = .31$, $p < .001$). Forest structural complexity increased with increasing absolute latitude ($r^2 = .26$, $p < .001$).

Main conclusions: Because large-diameter trees constitute roughly half of the mature forest biomass worldwide, their dynamics and sensitivities to environmental change represent potentially large controls on global forest carbon cycling. We recommend managing forests for conservation of existing large-diameter trees or those that can soon reach large diameters as a simple way to conserve and potentially enhance ecosystem services.

KEYWORDS
forest biomass, forest structure, large-diameter trees, latitudinal gradient, resource inequality, Smithsonian ForestGEO

1 | INTRODUCTION

Concentration of resources within a few individuals in a community is a pervasive property of biotic systems (West, Brown, & Enquist, 1997), whether marine (Hixon, Johnson, & Sogard, 2014), terrestrial (Enquist, Brown, & West, 1998) or even anthropogenic (Saez & Zucman, 2016). The concentration of total forest biomass in a few large-diameter trees is no exception (Pan, Birdsley, Phillips, & Jackson, 2013). Large-diameter trees in forests take many decades or even centuries to develop, but human or natural disturbances can decrease their abundance, rapidly changing forest structure (Allen et al., 2010; Lindenmayer, Laurance, & Franklin, 2012; Lutz, van Wagtendonk, & Franklin, 2009; van Mantgem et al., 2009).

Despite the recognized ecological significance of large-diameter trees within individual forest types, relatively little is known about the distribution and abundance of large-diameter trees at the global scale. Previous studies have showed that large-diameter trees comprise a large fraction of the biomass of many forests (Bastin et al., 2015; Brown et al., 1995; Clark & Clark, 1996; Lutz, Larson, Swanson, & Freund, 2012) and that they modulate stand-level leaf area, microclimate and water use (Martin et al., 2001; Rambo & North, 2009). Large-diameter trees contribute disproportionately to reproduction (van Wagtendonk & Moore, 2010), influence the rates and patterns of regeneration and succession (Keeton & Franklin, 2005), limit light and water available to smaller trees (Binkley, Stape, Bauerle, & Ryan, 2010), and contribute to rates and causes of mortality of smaller individuals by crushing or injuring sub-canopy trees when their bole or branches fall to the ground (Chao, Phillips, Monteagudo, Torres-Lezama, & Vásquez Martínez, 2009; Das, Stephenson, & Davis, 2016). Large-diameter trees (and large-diameter snags and large-diameter fallen woody debris) make the structure of primary forests and mature secondary forests unique (Spies & Franklin, 1991). Large-diameter trees occur at low stem densities, yet influence spatial patterns over long inter-tree distances (Das, Larson, & Lutz, 2018; Enquist, West, & Brown, 2009; Lutz et al., 2014). Consequently, to elucidate the patterns, mechanisms and consequences of large-diameter tree ecology requires sample plots $\geq$ 1 ha (Das, Battles, Stephenson, & van Mantgem, 2011; Lutz, 2015; Réjou-Méchain et al., 2014).

Changes in climate, disturbance regimes and logging are accelerating the decline of large-diameter trees (e.g., Bennett, McDowell, Allen, & Anderson-Teixeira, 2015; Lindenmayer & Laurence, 2016; Lindenmayer et al., 2012). The dynamics of large-diameter trees is dependent on at least two factors: (a) presence of species capable of attaining a large size, and (b) conditions, including disturbance regimes, that permit the development of large-diameter individuals. If the species richness of the large-diameter assemblage is high, a forest may be better able to respond to perturbations (Musavi et al., 2017) and maintain its structure and ecological function. However, if the large-diameter species richness is low, then a forest could be susceptible to any change that affected those few species.

Surprisingly, the specific roles of large-diameter trees are not well anchored in two widely referenced theories of global vegetation. Both the unified neutral theory of biodiversity (Hubbell, 2001) and metabolic scaling theory (West, Enquist, & Brown, 2009) propose that plants have a degree of functional equivalency. The unified neutral theory makes predictions about the rank-order abundance of species in a forest, but it makes no specific predictions about the rank order of large-diameter species or even if large-diameter individuals are members of common or rare species. Metabolic scaling theory does predict the abundance of large-diameter trees, and empirical tests of the theory for more abundant, smaller-diameter individuals are generally good. However, metabolic scaling theory often tends to under-predict the abundance of large-diameter trees in temperate forests (Anderson-Teixeira, McGarvey, et al., 2015; their fig. 2) and rather over-predict the abundance of large-diameter trees in tropical forests (Muller-Landau et al., 2006; their table 2) and in some temperate forests (Lutz et al., 2012; their fig. 2). Metabolic scaling theory also advances its predictions as continuous functions, and the departure from theory (i.e., the spatial variation) at discrete grain sizes remains unquantified. Accordingly, these theories alone cannot fully explain global patterns of forest species diversity or the larger portion of the size distribution (Coomes, Duncan, Allen, & Truscott, 2003; LaManna et al., 2017; Lutz et al., 2012; Muller-Landau et al., 2006).

However, studies do suggest that a greater generalization of forest structure in the tropical, subtropical, temperate and boreal forests of the world may indeed be possible (i.e., Gilbert et al., 2010; Ostertag, Inman-Narahari, Cordell, Giardina, & Sack, 2014; Slik et al., 2013). To the extent that forests share structural attributes either globally or regionally, our ability to model forest change may be improved by focusing on global patterns in structure rather than individual species life-history traits. We expected that latitudinal trends in the concentration of biomass in the largest trees would follow trends in forest

density (with more stems in the largest diameter classes, relative biomass should be higher). We also expected that relative richness of the large-diameter cohort would be lower in forests with high stem density because the large trees would be a smaller fraction of stems and thus a smaller fraction of species. Our principal hypothesis was that only a small proportion of the largest trees are responsible for the preponderance of forest biomass, and that the abundance and variation of these large-diameter trees reflect latitudinal gradients of forest structure. Specifically we set out to ask four interrelated questions:

1. Are there global relationships between large-diameter trees (defined various ways) and forest biomass?
2. Does the richness of the large-diameter cohort depend on the richness or biomass of the forest?
3. Are there latitudinal gradients in forest density, biomass, concentration of biomass, or structural complexity?
4. Are large-diameter trees members of common or rare species in forests?

2 | MATERIALS AND METHODS

We used data from the Forest Global Earth Observatory (ForestGEO; Anderson-Teixeira, Davies, et al., 2015) network of forest dynamics plots coordinated by the Smithsonian Institution, which includes major forest types in the Köppen climate zones of cold, temperate and tropical forests (Figure 1, Supporting Information Table S3.1). Forests included in the ForestGEO network include undisturbed primary forests or older secondary forests meeting the United Nations Food and Agricultural Organization definition of forest (trees $>$ 5 m tall and canopy cover $>$ 10% occurring in patches $>$ 0.5 ha; Forest Resource Assessment, 2015). The ForestGEO plots feature consistent field methods (Condit, 1998) and data representation (Condit, Lao, Singh, Esufali, & Dolins, 2014). Importantly, these plots include all standing woody stems $\geq$ 1 cm diameter at breast height (1.3 m along the main stem; DBH). A representativeness analysis showed that the ForestGEO includes most major forest types of the world, albeit with some exceptions (see Anderson-Teixeira, Davies, et al., 2015 for details). We analysed 48 plots in primary or older secondary forest spanning 86.4° of latitude (Figure 1), covering 1,278 ha (median size 24 ha), and including 5,601,473 stems representing 9,298 species and 210 plant families (Figure 1, Table 1, Supporting Information Table S3.1).

There is no universal definition for what constitutes a large-diameter tree. Generally, a large-diameter tree is of reproductive stature, is tall enough to reach the upper canopy layer of the forest, and is larger than the majority of woody stems in the forest. In any forest, the largest trees *relative to the rest of the stand* contribute disproportionately to ecological function and represent some of the longest-lived and most fecund components of their respective forests. The definition of large-diameter inherently depends on species and forest type. In cold, continental forests, a large-diameter tree may only be 20 cm DBH (Baltzer, Venes, Chasmer, Sniderhan, & Quinton, 2014). In productive temperate or tropical forests, a large-diameter tree may be $>$ 100 cm DBH (Lutz et al., 2012; Lutz, Larson, Freund, Swanson, & Bible, 2013). To compare dissimilar ecosystems, we used three metrics for defining large diameter trees:

1. 99th percentile diameter (the largest 1% of trees $\geq$ 1 cm DBH in the forest).
2. Fixed diameter. We used a fixed threshold for large-diameter trees of 60 cm DBH, a diameter reached by at least some trees in almost all plots.
3. The large-diameter threshold. We defined the large-diameter threshold to be that diameter such that trees greater than or equal to that diameter constituted half of the aboveground live biomass of the plot.

We calculated the density, basal area, and biomass of stems $\geq$ 1 cm DBH and tabulated them within each square hectare (100 m $\times$ 100 m)

FIGURE 1 Location of the 48 plots affiliated with the Smithsonian Forest Global Earth Observatory (ForestGEO) used in this study

of the 48 plots. Because the distribution of large-diameter trees within forests is often not homogeneous (e.g., Lutz et al., 2013), we used the 1-ha scale to capture variation in structure across the plots without introducing the spurious high or low values of biomass that could be associated with small extents (Réjou-Méchain et al., 2014). We calculated biomass for tropical forests (absolute latitude $\leq$ 23.5°) by the methods of Chave et al. (2014), which uses a generic equation to predict biomass based on diameter, climate and wood density. The Chave et al. (2014) equations are of the form:

$$AGB = \exp[-1.803 - 0.976E + 0.976\ln(\rho) + 2.676\ln(DBH) - 0.0299\ln(DBH)^2] \quad (1)$$

where ρ is wood density and E is the environmental parameter. Wood specific gravity was taken from Zanne et al. (2009), and we used the values hierarchically, taking species-specific values where defined, then genus-specific values, then family-specific values. If there was no wood specific gravity data for the plant family, or if the stem was unidentified, we used the global average of 0.615 g/cm^3. Values for the environmental parameter E are listed in Supporting Information Table S3.1.

We calculated biomass for cold and temperate plots (absolute latitude $>$ 23.5°) using the composite taxa-specific equations of Chojnacky, Heath, & Jenkins (2014). Those equations are of the form

$$\ln(\text{biomass}) = \beta_0 + \beta_1 \times \ln(\text{DBH}) \quad (2)$$

where β_0 and β_1 are listed in Chojnacky et al. (2014; their table 5).

Species not represented by specific biomass equations were defaulted to an equation or wood density value for the genus or the family. We used site-specific allometric equations for Palamanui (Ostertag et al., 2014), Laupahoehoe (Ostertag et al., 2014), Lanjenchi (Aiba & Nakashizuka, 2009) and Changbaishan (Wang, 2006).

We further analysed the diameter–abundance relationships of each plot based on six tree diameter classes (1 cm $\leq$ DBH $<$ 5 cm, 5 cm $\leq$ DBH $<$ 10 cm, 10 cm $\leq$ DBH $<$ 30 cm, 30 cm $\leq$ DBH $<$ 60 cm, 60 cm $\leq$ DBH $<$ 90 cm and DBH $\geq$ 90 cm). Diameter classes were selected to include recognized differences in tree life-history traits (Memiaghe, Lutz, Korte, Alonso, & Kenfack, 2016). We performed non-metric multidimensional scaling (NMDS; Kenkel & Orloci, 1986) analyses on the density of each diameter class of each 100 m $\times$ 100 m area. We used the Bray–Curtis dissimilarity index and performed the NMDS ordinations in three dimensions using the version 2.4-4 of the vegan package (Oksanen, Kindt, & Simpson, 2016) in R version 3.3.1 (R Development Core Team, 2016). We used the three-dimensional coordinates of each 1-ha in NMDS space to create a metric for structural complexity. For the 1-ha structural ordination values for each plot, we fit a one standard deviation ellipsoid using the orglellipse function from the vegan3d package (Oksanen, 2017). We then calculated the volume of that ellipsoid as a metric of structural difference (i.e., complexity) to compare the relative differences between 100 m $\times$ 100 m areas within the plot.

To examine commonness of species that can reach large diameters, we ranked all species according to their abundance within each plot. We then identified large-diameter species as species that had $\geq$ 1 individual with a DBH greater than or equal to the large-diameter threshold, and determined the species rank for each of these large-diameter species (i.e., if the third most abundant species was a 'large-diameter species', it would receive rank = 3). We then used the median rank for all large-diameter species ranks within each plot, and normalized this value across plots by dividing rank by the total number of species (i.e., in a plot with 60 species, a median rank of 18 becomes 0.3).

To validate our results, we calculated structural accumulation curves for each plot, calculating the area required to estimate forest density and aboveground live biomass to within 5% of the entire plot value. Within each plot, for each of density and biomass, we used random sampling of 400 m^2 quadrats with replacement (from the available quadrats), beginning with a random sample of $n = 1$ quadrat and ending with a random sample of n = total number of quadrats in each plot. This process was repeated based on the number of quadrats in each plot, which allowed us to calculate a mean and standard deviation for each value of n. A percent deviation metric was calculated as:

$$\text{Percent difference} = \left(\text{abs}\left(\text{mean}_n - \text{mean}_{\text{plot}}\right) + SD_n\right)/\text{mean}_{\text{plot}} \quad (3)$$

where mean_n is the mean of a random sampling of n quadrats, $\text{mean}_{\text{plot}}$ is the mean for the entire plot, and SD_n is the standard deviation for the random sample of n quadrats.

3 | RESULTS

Average stem density in the plots ranged from 608 stems/ha (Mudumalai, India) to 12,075 stems/ha (Lanjenchi, Taiwan) with most high-density plots occurring in the tropics (Tables 1 and 2, plot characteristics in Table S3.1 and Appendix). Aboveground live tree biomass ranged from 13 Mg/ha (Mpala, Kenya) to 559 Mg/ha (Yosemite, USA). The biomass of trees $\geq$ 60 cm DBH ranged from 0 Mg/ha (Mpala, Kenya, Palamanui, USA, and Scotty Creek, Canada) to 447 Mg/ha (Yosemite, USA). The large-diameter tree threshold (separating the plot aboveground forest biomass into two equal parts) varied from 2.5 cm (Palamanui, USA) to 106.5 cm (Yosemite, USA). Variation in the abundance of trees of different diameter classes at the 1-ha scale was high globally (Supporting Information Tables S3.2 and S3.3), and coefficient of variation (CV) of the 1-ha stem densities was highest in the cold temperate/boreal plots and lowest in the tropics (Table 2).

There was a strong positive relationship between the large-diameter threshold and overall forest biomass ($r^2 = .62$, $p < .001$; Figure 2a). This relationship held for all three of our definitions for large-diameter trees (Figure 2a–c). The relationship for large-diameter threshold was strongest, but the biomass of the largest 1% of trees also predicted total biomass ($r^2 = .35$, $p < .001$; Figure 2b) as did the density of stems $\geq$ 60 cm DBH ($r^2 = .49$, $p < .001$; Figure 2c). Results based on basal area were similar to those for biomass (Supporting Information Figure S1.1). There was a negative relationship between large-diameter species richness and total biomass ($r^2 = .45$, $p < .001$; Figure 2d), which was consistent with the negative relationship between large-diameter threshold and large-diameter richness ($r^2 = .33$, $p < .001$; Figure 2e) and the negative relationship between large-diameter richness and the biomass of the largest 1% of trees ($r^2 = .61$, $p < .001$; Figure 2f). In other words, plots with high biomass

TABLE 1 Structural characteristics of global forests

Plot	Large-diameter threshold (cm)	Density (stems/ha) (*SD*)	Biomass (Mg/ha) (*SD*)	Total species (*n*)	Large-diameter species (*n*)	Large-diameter richness (%)	Biomass of the 1% (%)	Density ≥ 60 cm DBH (stems/ha)
Yosemite	106.5	1399 (266)	559 (130)	14	3	21	46	52
Wind River	92.9	1207 (273)	532 (161)	26	5	19	33	72
Žofín	78.0	2404 (982)	248 (66)	11	4	36	56	41
Ituri Lenda	72.0	7553 (829)	467 (62)	396	25	6	83	34
Danum Valley	65.7	7573 (526)	486 (152)	784	62	8	72	27
SERC[a]	65.4	2086 (792)	299 (49)	79	25	32	40	40
Laupahoehoe	63.4	3925 (859)	241 (45)	22	2	9	58	37
Santa Cruz[a]	62.3	1945 (593)	361 (102)	31	7	23	41	34
Cocoli	60.1	2164 (248)	281 (37)	170	9	5	59	32
Huai KhaKhaeng	59.9	2506 (674)	258 (65)	284	80	28	57	20
SCBI[a]	59.7	1850 (1637)	259 (43)	64	22	34	31	35
Ituri Edoro	59.3	8956 (1270)	375 (46)	426	63	15	80	23
Changbaishan	56.2	1230 (188)	288 (33)	52	15	29	22	34
Bukit Timah	55.6	6273 (180)	363 (140)	353	18	5	73	19
Rabi	54.7	7988 (926)	323 (74)	346	74	21	73	14
Lambir	51.9	7635 (1233)	495 (99)	1387	223	16	69	27
Barro Colorado	51.2	4938 (463)	257 (49)	297	80	27	67	17
Lilly Dickey[a]	51.2	1112 (441)	214 (29)	34	19	56	22	20
Xishuangbanna	49.8	4565 (650)	280 (81)	450	93	21	57	19
Wanang	49.6	5523 (520)	324 (61)	581	170	29	61	14
Palanan	49.4	4981 (489)	414 (119)	324	41	13	62	27
Pasoh	48.5	5735 (631)	324 (55)	926	194	21	63	13
Michigan Woods	47.5	1981 (515)	192 (25)	44	16	36	26	14
Tyson[a]	45.4	1601 (751)	176 (16)	45	18	40	24	10
Wytham Woods[a]	44.8	1016 (309)	310 (46)	23	13	57	23	18
Korup	42.9	7283 (920)	345 (88)	485	143	29	67	10
Manaus	42.2	6234 (441)	344 (54)	1529	260	17	59	9
Cedar Breaks	41.9	1542 (961)	168 (53)	17	8	47	34	13
Mudumalai	41.7	608 (210)	205 (33)	72	35	49	18	12
Jianfengling	40.8	6526 (993)	392 (37)	290	116	40	48	24
La Planada	40.8	4030 (243)	270 (30)	241	74	31	43	8
Fushan	39.2	4478 (1139)	224 (25)	106	33	31	46	14
Sherman	38.5	3662 (550)	275 (41)	224	31	14	53	13
Amacayacu	37.6	4948 (518)	268 (33)	1233	326	26	49	7
Kenting	36.1	3760 (410)	255 (38)	92	40	43	36	7
Lienhuachih	35.7	6131 (1760)	170 (25)	145	49	34	51	10
Harvard Forest[a]	35.5	3104 (2600)	260 (66)	55	17	31	23	7
Luquillo	35.5	2903 (626)	283 (53)	133	47	35	39	12

(Continues)

TABLE 1 (Continued)

Plot	Large-diameter threshold (cm)	Density (stems/ha) (*SD*)	Biomass (Mg/ha) (*SD*)	Total species (*n*)	Large-diameter species (*n*)	Large-diameter richness (%)	Biomass of the 1% (%)	Density ≥ 60 cm DBH (stems/ha)
Heishiding	34.5	5277 (706)	149 (27)	213	59	28	43	12
Wabikon[a]	31.1	1692 (1017)	111 (14)	31	15	48	17	1
Gutianshan	31.0	5833 (1580)	185 (27)	159	40	25	34	2
Ilha do Cardoso	31.0	4660 (578)	148 (17)	135	43	32	41	7
Yasuni	29.1	5834 (692)	261 (48)	1075	343	32	50	8
Hong Kong[a]	28.6	5860 (1056)	142 (20)	172	43	25	39	3
Lanjenchi	17.2	12075 (2795)	113 (7)	128	72	56	29	1
Mpala	10.0	2963 (2902)	13 (8)	68	35	51	30	0
Scotty Creek	7.6	4136 (1407)	22 (11)	11	7	64	15	0
Palamanui	2.5	8205 (1084)	30 (5)	16	11	69	13	0

Note. Values for density and biomass include trees ≥ 1 cm diameter at breast height (DBH) within each square hectare (100 m × 100 m) of the plots, with the mean and *SD* calculated for each full hectare. The large-diameter threshold represents the diameter where half the biomass is contained within trees above that threshold. The biomass of the 1% indicates the proportion of total live aboveground tree biomass contributed by the largest 1% of trees ≥ 1 cm DBH. Plots are listed by declining large-diameter threshold. For additional details of the plots and forest characteristics, see Supporting Information Tables S3.1-S3.3 and references in the Appendix.

[a]Mature secondary forest. SERC - Smithsonian Environmental Research Center; SCBI - Smithsonian Conservation Biology Institute.

had high large-diameter thresholds and relatively low species richness within this large-diameter structural class.

The amount of aboveground forest biomass contained within the largest 1% of trees averaged among the 48 plots was 50% (weighted by the forest biomass of each plot, 45% as an unweighted average of the 48 plots), representing an average of 23% of the total species richness (Table 1). The average large-diameter threshold was 47.7 cm DBH (half of the biomass of the 48 plots was contained within trees ≥ 47.7 cm DBH). The average portion of biomass contained within trees ≥ 60 cm DBH in the 48 plots was 41%. Forest density gradually decreased with increasing absolute latitude ($r^2 = .31$, $p < .001$; Figure 3a), as did the proportion of tree biomass accounted for by the largest 1% of trees ($r^2 = .46$, $p < .001$; Figure 3c), following our expectations and partially a reflection of the higher stem densities in the tropics (Figure 3a, Table 1, Supporting Information Table S3.2). However, latitudinal gradients were not present for biomass (Figure 3b) or the large-diameter threshold (Figure 3d).

The three metrics for large-diameter trees were not perfectly correlated (Supporting Information Figure S1.2). The large-diameter threshold and the density of stems ≥ 60 cm DBH had a linear relationship ($r^2 = .80$, $p < .001$), even though some forests did not have trees ≥ 60 cm DBH. The relationship between the biomass of the 1% of largest diameter trees and both the density of stems ≥ 60 cm DBH and the large-diameter threshold was significant for tropical plots but not for temperate plots.

NMDS ordinations of the abundance of trees in the six diameter classes in each 100 m × 100 m area showed that tropical forests have a higher degree of structural similarity than temperate or boreal forests

TABLE 2 The effect of geographical region on tree density and biomass and their variation at 1-ha scale and the abundance of large-diameter trees as measured by the three metrics of proportion of biomass in the largest 1% of trees, density of trees ≥ 60 cm diameter at breast height (DBH), and large-diameter threshold

Zone	Plots (*n*)	Density (trees/ ha)	Density *SD*	Density CV	Biomass (Mg/ha)	Biomass *SD*	Biomass CV	Biomass of the 1% (%)	Density trees ≥ 60 cm DBH (trees/ha)	Large-diameter threshold (cm)
Cold temperate/boreal	6	2,281	1,114	47	174	98	24	23	11	37
Temperate	16	3,339	2,193	31	266	126	18	38	24	53
All Tropics	26	5,735	1,072	18	278	57	20	61	16	44
Tropical Africa	5	6,949	2,317	29	305	172	27	76	16	48
Tropical Asia	10	5,767	3,149	16	330	124	21	53	18	47
Tropical Latin America	8	4,339	1,410	12	280	27	15	54	13	42
Tropical Oceania	3	5,884	2,162	15	198	152	18	61	17	38

SD = standard deviation; CV = coefficient of variation.

Note. The *SD* of density and the *SD* of biomass represent the within-region (between-plot) variation. The CV of density and CV of biomass represent the average of the individual plot 1-ha CVs, with each plot weighted equally.

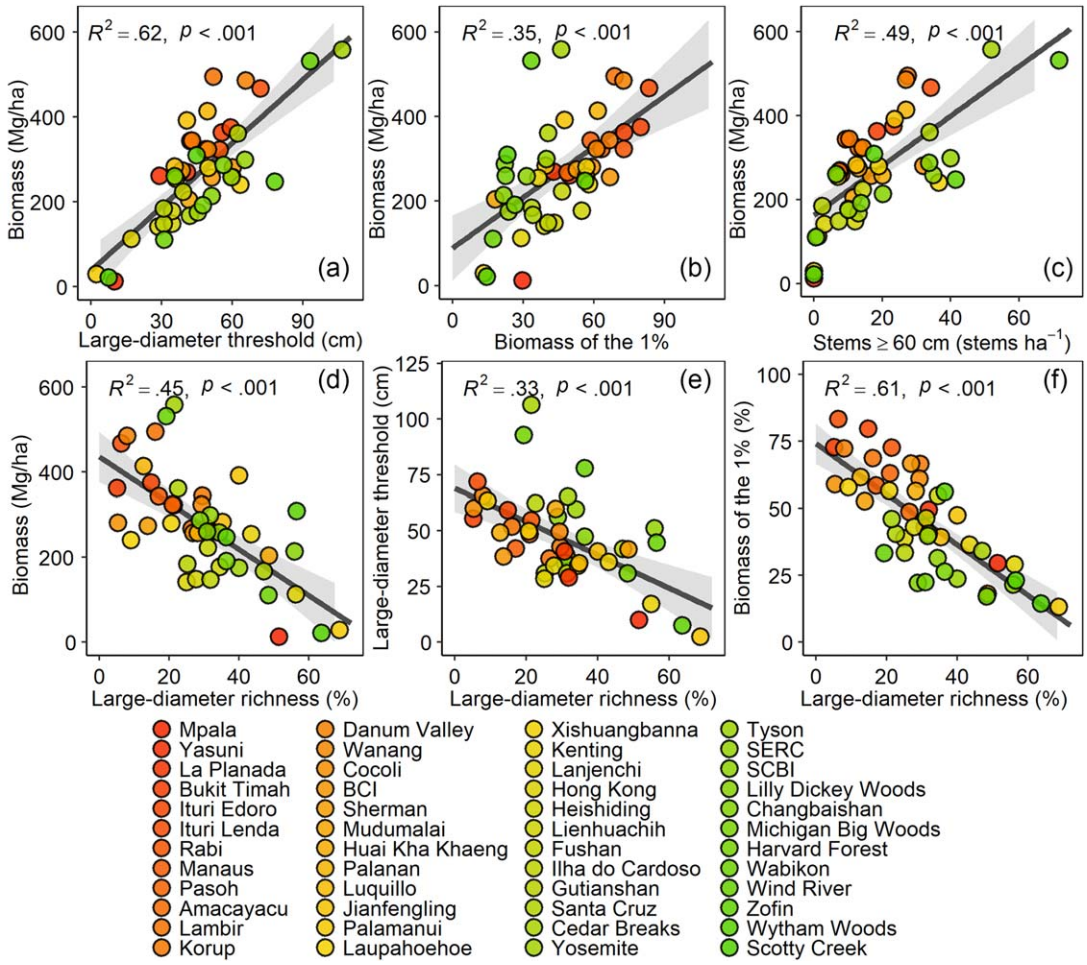

FIGURE 2 Contribution of large-diameter trees to forest structure of 48 large forest plots. Aboveground live tree biomass increases with increasing large-diameter threshold (a). The large-diameter threshold reflects the tree diameter that segments biomass into two equal parts. Below the large-diameter threshold are a large number of small-diameter trees, and above the large-diameter threshold are a smaller number of large-diameter trees. Aboveground live biomass also increases with the concentration of biomass in the largest 1% of trees (b) and the density of stems ≥ 60 cm diameter at breast height (DBH; c). Large-diameter richness declines with increasing biomass (d), which is consistent with the declining relationship between large-diameter threshold and large-diameter richness (e). The concentration of biomass in the largest 1% of trees has a strong negative relationship with large-diameter richness (f). Colours indicate increasing absolute latitude from red to green. Grey areas around regression lines indicate 95th percentile confidence intervals

based on their position in the ordination (Figure 4a,b). The 1-ha scale variation for tropical plots also showed a high degree of similarity both globally (clustering and high overlap of red ellipses in Figure 4c,d) and locally (smaller size of individual red ellipses). The volumes occupied by the 1-ha NMDS points of temperate plots, conversely, covered a wide range in ordination space, indicating greater structural variability both among and within the plots (greater size and dispersion of green ellipses in Figure 4c,d, three-dimensional animation in Supporting Information Figure S2). This phenomenon was also mirrored by coefficients of variation of density and biomass of 1-ha quadrats, which differed among regions and were higher in temperate and boreal forests than in tropical plots (Table 2). The grouping of plots with no trees ≥ 60 cm DBH (left of Figure 4a,b; Supporting Information Table S3.2) shows a structural equivalency of forests growing in stressful environments. Those forests include Scotty Creek, Canada (temperature, nitrogen and hydrologically limited), Mpala, Kenya (water and herbivory limited) and Palamanui, USA (water limited, limited soil development and with limited species complement). The structural complexity of forests (variation in abundance of the six diameter classes) at 1-ha scale increased with increasing absolute latitude (Figure 5a).

Large-diameter trees consisted primarily of common species (rank < 0.5; Figure 5b), and rarer species reached large diameter in plots with higher large-diameter richness (r^2 = .17; p = .002). The absolute numbers of species that reached the local large-diameter threshold ranged from two in tropical Laupahoehoe, USA, to 343 in Yasuni, Ecuador (Table 1). Tropical plots generally had > 25 species reaching the large-diameter threshold (minimum nine species in Cocoli, Panama). Temperate plots generally had < 10 species that reached the large-diameter threshold (maximum 25 species in Smithsonian Ecological Research Center (SERC), USA). On a percentage basis, large-diameter richness ranged from 5% (Cocoli, Panama and Bukit Timah, Singapore) to 69% (Palamanui, USA). The relative

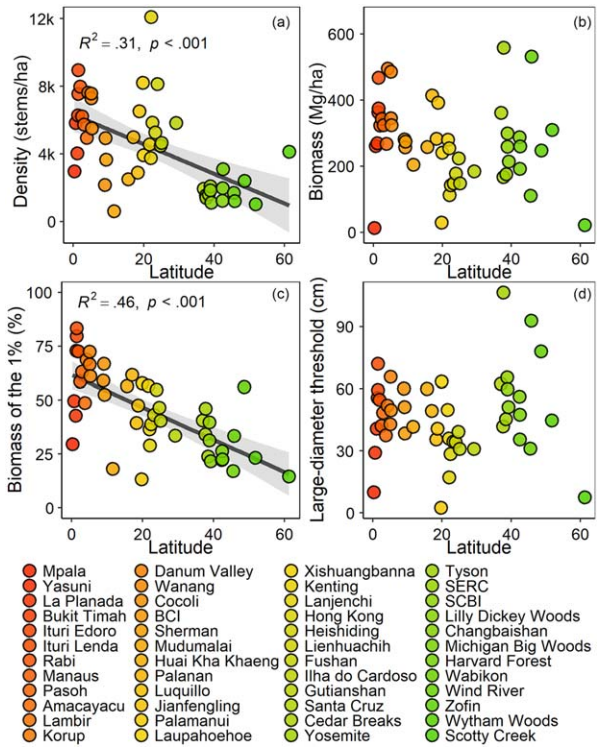

FIGURE 3 Gradients of forest structural attributes by absolute latitude for 48 forest plots in the ForestGEO network. Absolute latitudinal gradients in density (a) and concentration of biomass in the largest 1% of trees (c) were significant. The relationships for biomass (b; $r^2 = .04$, $p = .106$) and the large-diameter threshold (d; $r^2 = .01$, $p = .551$) were not. Colours indicate increasing absolute latitude from red to green. Grey areas around regression lines indicate 95th percentile confidence intervals

richness of the large-diameter assemblage was highest in plots with low biomass, while plots with high biomass had a lower proportion of richness represented by the large-diameter trees (Figure 2d, Table 1). In general, forests with lower total richness had a higher proportion of that richness retained in the large-diameter class. Unsurprisingly, plots with lower large-diameter thresholds (< 60 cm DBH) had a higher proportion of species represented in the large-diameter assemblage (mean 34%), whereas plots with large-diameter thresholds ≥ 60 cm DBH had a lower proportion of species represented in the large-diameter guild (mean 18%).

4 | DISCUSSION

The relationship between the large-diameter threshold and overall biomass (Figure 2a) suggests that forests cannot sequester large amounts of aboveground carbon without large trees, irrespective of the richness or density of large-diameter trees. Species capable of attaining large diameters are relatively few (Figure 2) but individuals of these species are relatively abundant (Figure 5b). The relationships among biomass and richness across plots held over a range of stem densities (608 to 12,075 stems/ha) and among trees of varying wood densities (0.10 to 1.08 g/cm^3). A linear relation of biomass to large-diameter threshold (Figure 2a) best explained the correlation among the 48 plots, although we would expect an upper limit based on maximum tree heights (Koch, Sillett, Jennings, & Davis, 2004) or biomass (Sillett, Van Pelt, Kramer, Carroll, & Koch, 2015; Van Pelt, Sillett, Kruse, Freund, & Kramer, 2016). The generally high proportion of biomass represented by the largest 1% of trees reinforces the importance of these individuals to carbon sequestration and productivity (e.g., Stephenson et al., 2014). Larger numbers of small- and medium-diameter trees cannot provide equivalent biomass to a few large-diameter trees, although small and medium sized trees can contribute significantly to carbon cycling (Fauset et al., 2015; Meakem et al., 2017). The implication from scaling theory (West et al., 2009) is that large-diameter trees are taller and have heavier crowns, and occupy growing space not available to smaller trees (i.e., at the top of the canopy; Van Pelt et al., 2016; West et al., 2009).

Temperate forests featured a higher density of trees ≥ 60 cm DBH (Table 1), consistent with the presence of the very largest species of trees in cool, temperate forests (Sillett et al., 2015; Van Pelt et al., 2016). Temperate forests also exhibited considerably lower densities of small trees (e.g., 1 cm ≤ DBH < 5 cm; Supporting Information Table S3.2) and lower total stem density. In tropical forests, high overall stem densities are mostly due to trees with diameters ≤ 10 cm DBH (Table 2, Supporting Information Table S3.2). Metabolic scaling theory does predict the diameter–abundance relationship throughout much of the middle of the diameter range in many forest types (Anderson-Teixeira, McGarvey, et al., 2015; Lutz et al., 2012; Muller-Landau et al., 2006). However, the dichotomy between temperate forests and tropical forests, where temperate forests have lower densities of small trees and higher densities of large trees (and tropical forests the reverse), reinforces the need to examine departures from the theory's predictions. In tropical forests, the lower proportional richness of large-diameter trees likely has at least two explanations. First, tropical forests contain many more stems per ha (Supporting Information Table S3.2) with much higher small-diameter understorey diversity (LaFrankie et al., 2006). Secondly, not all of the species capable of reaching large diameters in that region may be present even in the large ForestGEO plots, and thus even the extensive ForestGEO network may have sampling limitations.

The grouping of plots with only small-diameter trees (Figure 4a) shows that forests in markedly different environments can exhibit convergent structure based on different limiting factors. Large-diameter trees can be abundant in any region (Supporting Information Table S3.1), but different factors may limit the ability of an ecosystem to support a high level of aboveground live biomass. In addition to environmental limits, ecosystems that are environmentally quite productive in terms of annual growth may be limited by frequent, severe disturbance (e.g., typhoons in Fushan and hurricanes in Luquillo). Finally, the regional species pool may not contain species that can attain large diameters in the local combination of climate and resource availability (e.g., Palamanui, USA). The higher levels of structural complexity at 1-ha scales in temperate forests may be due to higher proportions of the forests where small trees predominate and large-diameter trees are

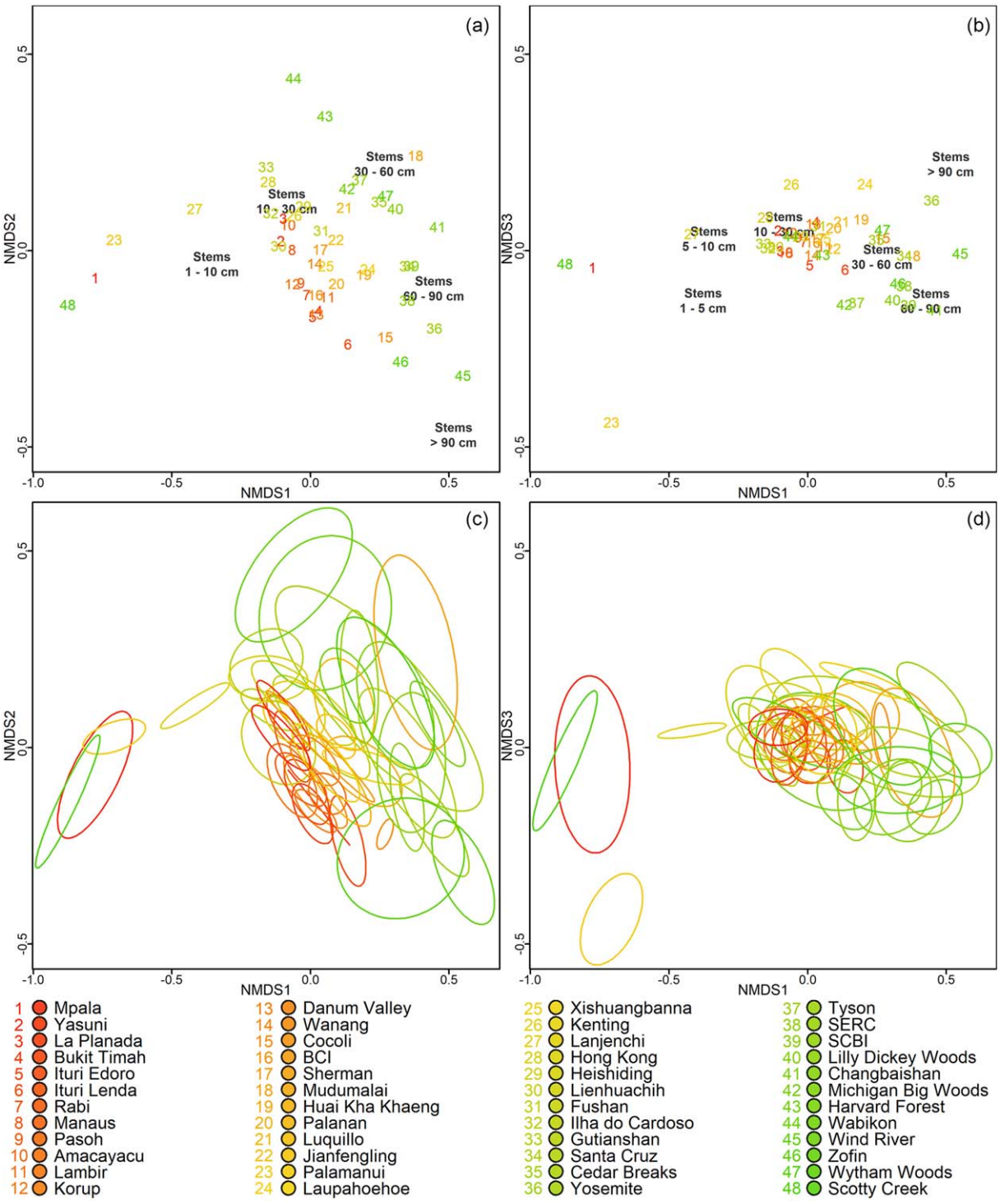

FIGURE 4 Three-dimensional non-metric multidimensional scaling (NMDS) results for density of trees organized into six diameter classes in 1260, 100 m × 100 m hectares of 48 forest plots in the ForestGEO network (a, b). The structural classes (diameter bins) used in the NMDS ordination are superimposed in black text (a, b). The within-plot variation in structure for each plot is shown by depiction of the *SD* ellipses of the individual 100 m × 100 m hectares within each plot [c, d; where (c) reflects the variation of NMDS1 versus NMDS2 (a) and (d) reflects the variation of NMDS1 versus NMDS3 (b)]. Ordination stress = 0.047. Colours indicate increasing absolute latitude from red to green, with plot centroids numbered (a, b). See Supporting Information Figure S2 for a three-dimensional animation of the structural ordination

generally excluded (i.e., swamps, rocky outcrops), supported by the higher coefficient of variation of density in temperate and cold forests (Table 2). The trend of increasing structural complexity (i.e., 1-ha heterogeneity) with increasing absolute latitude (Figure 5a) may in fact be hump-shaped, with decreasing complexity at higher latitudes than the 61.3°N of the Scotty Creek, Canada, plot.

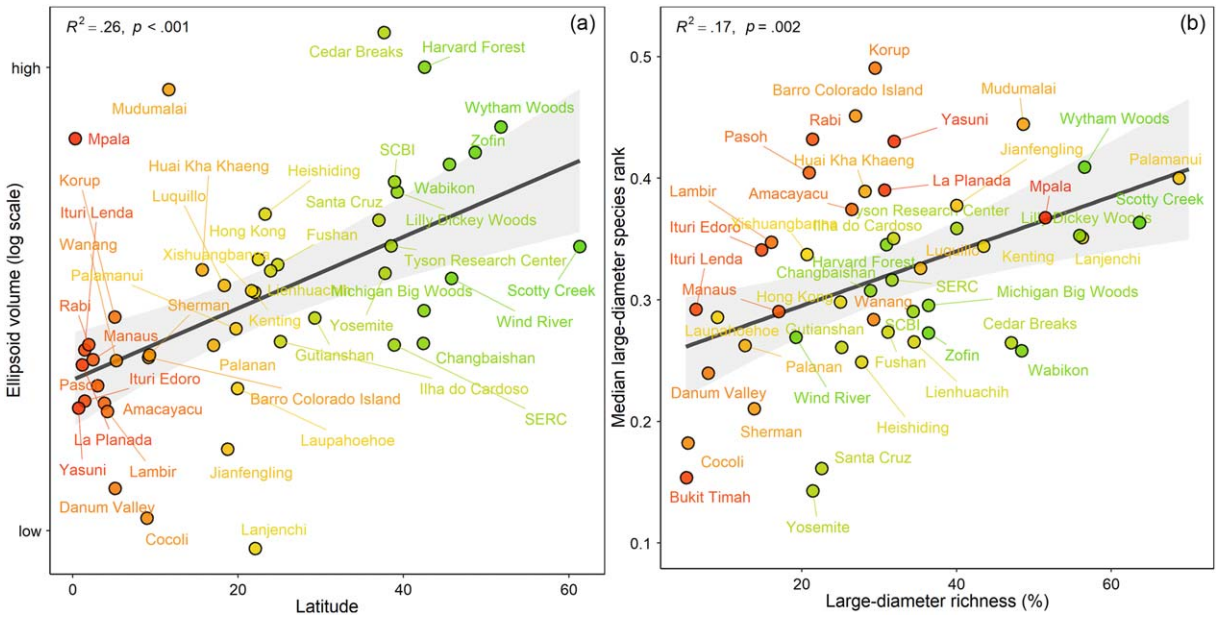

FIGURE 5 The 1-ha scale structural complexity of 48 forest plots in the ForestGEO network as a function of absolute latitude (a). The metric of structural complexity is the volume of the three-dimensional ellipsoid generated from the non-metric multidimensional scaling (NMDS) ordination of abundance in structural classes (see Figure 4 for two-dimensional projections and Supporting Information Figure S2 for a three-dimensional animation). The rank order of large-diameter species in 48 forest plots (b). Rank order is normalized to the range from zero to one to compare plots with differing species richness. Lower proportions of large-diameter species rank correspond to more abundant species (median large-diameter species rank < 0.5 for all 48 forest plots). Species attaining large-diameters were the more common species in the forest plots. Colours indicate increasing absolute latitude from red to green

There is still considerable uncertainty as to what will happen to large-diameter trees in the Anthropocene when so much forest is being felled for timber and farming, or is being affected by climate change. Bennett et al. (2015) suggested that the current large-diameter trees are more susceptible to drought mortality than smaller-diameter trees. Larger trees, because of their height, are susceptible to sapwood cavitation and are also exposed to high radiation loads (Allen, Breshears, & McDowell, 2015; Allen et al., 2010), but vigorous large-diameter individuals may also still be sequestering more carbon than smaller trees (Stephenson et al., 2014). Both Allen et al. (2015) and Bennett et al. (2015) suggested that larger trees will be more vulnerable to increasing drought than small trees, and Luo and Chen (2013) suggested that although the rate of mortality of larger trees will continue to increase because of global climate change, smaller trees will experience more drought-related mortality. These last two conclusions need not be in conflict as the background mortality rates for smaller trees are higher than those of larger trees within mature and old-growth forests (Larson & Franklin, 2010). What remains generally unanswered is whether the increasing mortality rates of large-diameter trees will eventually be offset by regrowth of different individuals of those same (or functionally similar) species. Any reduction in temperate zone large-diameter tree abundance may be compounded by the low large-diameter tree diversity in temperate forests (temperate forests had high relative large-diameter richness, but low absolute large-diameter richness). Large-diameter tree richness in tropical forests suggests more resilience to projected climate warming in two ways. First, absolute large-diameter tree richness was highest in tropical forests, suggesting that the large-diameter tree guild may have different adaptations that will allow at least some species to persist (Musavi et al., 2017). Secondly, the pool of species that can reach large diameters may have been undersampled in the plots used here, implying an even higher level of richness may exist in some forests than captured in these analyses.

The finding that large-diameter trees are members of common species groups (Figure 5b) contradicts the neutral theory's assumption of functional equivalency (Hubbell, 2001). Similarly the different structural complexity of forests worldwide (Figure 5a) contradicts the assumptions of universal size–abundance relationships of metabolic scaling theory (Enquist et al., 1998, 2009). The presence of a latitudinal gradient in forest density (Figure 3a) and the lack of a latitudinal gradient in forest biomass (Figure 3b) suggest that size–abundance relationships are not universal but depend on region or site conditions (Table 2).

Characterizing forest structural variation did require these large plots (Supporting Information Figure S1.3), a finding consistent with other studies examining forest biomass (Réjou-Méchain et al., 2014). With large plot sizes and global distribution, ForestGEO is uniquely suited to capture structural variation (i.e., the heterogeneity in the abundance of trees of all diameter classes). The relatively large area required (6.5 ha, on average) to estimate biomass to within 5% of the entire plot value reinforces conclusions that the distribution of large-diameter trees is not homogeneous within forests (e.g., Table 2; Furniss, Larson, & Lutz, 2017; Lutz et al., 2012, 2013). We note that this

calculation of the size of the plot required is a measure of spatial variation within the forest, and does not depend on the accuracy of the allometric equations used for calculating each tree's biomass. Allometric equations can be imprecise for large-diameter trees, both because of their structural variability and the enormous sampling effort, and therefore our estimates of overall biomass could be off by ± 15% (Lutz et al., 2017).

Although temperate plots had much lower overall species diversity compared to the tropical plots, tropical plots had much more homogeneous structure, both within and across plots (Figure 4), potentially suggesting greater structural equivalency among the many species present. We found that the largest 1% of trees constitute 50% of the biomass (and hence, carbon), supporting our hypothesis of their significance, at least in primary forests or older secondary forests. The conservation of large-diameter trees in tropical and temperate forests is therefore imperative to maintain full ecosystem function, as the time necessary for individual trees to develop large sizes could preclude restoration of full ecosystem function for centuries following the loss of the oldest and largest trees (Lindenmayer et al., 2012). Clearly, areas that have been recently logged lack large-diameter trees, and therefore have less structural heterogeneity than older forests. That the largest individuals belong to relatively few common species in the temperate zone means that the loss of large-diameter trees could alter forest function – if species that can attain large diameters disappear, forests will feature greatly reduced structural heterogeneity (e.g., Needham et al., 2016), biomass, and carbon storage. In the tropical zones, the larger absolute numbers of species reaching large diameters may buffer those forests against structural changes. Policies to conserve the tree species whose individuals can develop into large, old trees (Lindenmayer et al., 2014) could promote retention of aboveground biomass globally as well as maintenance of other ecosystem functions.

ACKNOWLEDGMENTS

Funding for workshops during which these ideas were developed was provided by NSF grants 1545761 and 1354741 to SD Davies. This research was supported by the Utah Agricultural Experiment Station, Utah State University, and approved as journal paper number 8998. Acknowledgements for the global support of the thousands of people needed to establish and maintain these 48 plots can be found in Supporting Information Appendix S4. References to locations refer to geographical features and not to the boundaries of any country or territory.

DATA ACCESSIBILITY

Data for plots in the ForestGEO network are available through the online portal at: http://www.forestgeo.si.edu

ORCID

James A. Lutz http://orcid.org/0000-0002-2560-0710
Tucker J. Furniss http://orcid.org/0000-0002-4376-1737
Daniel J. Johnson http://orcid.org/0000-0002-8585-2143
Alfonso Alonso http://orcid.org/0000-0001-6860-8432
Kristina J. Anderson-Teixeira http://orcid.org/0000-0001-8461-9713
Kendall M. L. Becker http://orcid.org/0000-0002-7083-7012
Erika M. Blomdahl http://orcid.org/0000-0002-2614-821X
Kuo-Jung Chao http://orcid.org/0000-0003-4063-0421
Sara J. Germain http://orcid.org/0000-0002-5804-9793
Keping Ma http://orcid.org/0000-0001-9112-5340
Jonathan A. Myers http://orcid.org/0000-0002-2058-8468
Perry Ong http://orcid.org/0000-0002-1597-1921
Richard P. Phillips http://orcid.org/0000-0002-1345-4138
Xugao Wang http://orcid.org/0000-0003-1207-8852

REFERENCES

Aiba, M., & Nakashizuka, T. (2009). Architectural differences associated with adult stature and wood density in 30 temperate tree species. *Functional Ecology*, *23*, 265–273.

Allen, C. D., Breshears, D. D., & McDowell, N. G. (2015). On underestimation of global vulnerability to tree mortality and forest die-off from hotter drought in the Anthropocene. *Ecosphere*, *6*, art129–art155.

Allen, C. D., Macalady, A. K., Chenchouni, H., Bachelet, D., McDowell, N., Vennetier, M., … Cobb, N. (2010). A global overview of drought and heat-induced tree mortality reveals emerging climate change risks for forests. *Forest Ecology and Management*, *259*, 660–684.

Anderson-Teixeira, K. J., Davies, S. J., Bennett, A. C., Gonzalez-Akre, E. B., Muller-Landau, H. C., Wright, S. J., … Zimmerman, J. (2015). CTFS-ForestGEO: A worldwide network monitoring forests in an era of global change. *Global Change Biology*, *21*, 528–549.

Anderson-Teixeira, K. J., McGarvey, J. C., Muller-Landau, H. C., Park, J. Y., Gonzalez-Akre, E. B., Herrmann, V., … McShea, W. J. (2015). Size-related scaling of tree form and function in a mixed-age forest. *Functional Ecology*, *29*, 1587–1602.

Baltzer, J. L., Venes, T., Chasmer, L. E., Sniderhan, A. E., & Quinton, W. L. (2014). Forests on thawing permafrost: Fragmentation, edge effects, and net forest loss. *Global Change Biology*, *20*, 824–834.

Bastin, J.-F., Barbier, N., Réjou-Méchain, M., Fayolle, A., Gourlet-Fleury, S., Maniatis, D., … Bogaert, J. (2015). Seeing central African forests through their largest trees. *Scientific Reports*, *5*, 13156.

Bennett, A. C., McDowell, N. G., Allen, C. D., & Anderson-Teixeira, K. J. (2015). Larger trees suffer most during drought in forests worldwide. *Nature Plants*, *1*, 15139.

Binkley, D., Stape, J. L., Bauerle, W. L., & Ryan, M. G. (2010). Explaining growth of individual trees: Light interception and efficiency of light use by Eucalyptus at four sites in Brazil. *Forest Ecology and Management*, *259*, 1704–1713.

Brown, I. F., Martinelli, L. A., Thomas, W. W., Moreira, M. Z., Cid Ferreira, C. A., & Victoria, R. A. (1995). Uncertainty in the biomass of Amazonian forests: An example from Rondônia, Brazil. *Forest Ecology and Management*, *75*, 175–189.

Chao, K.-J., Phillips, O. L., Monteagudo, A., Torres-Lezama, A., & Vásquez Martínez, R. (2009). How do trees die? Mode of death in northern Amazonia. *Journal of Vegetation Science*, *20*, 260–268.

Chave, J., Réjou-Méchain, M., Búrquez, A., Chidumayo, E., Colgan, M. S., Delitti, W. B. C., … Vieilledent, G. (2014). Improved allometric models to estimate the aboveground biomass of tropical trees. *Global Change Biology*, *20*, 3177–3190.

Chojnacky, D. C., Heath, L. S., & Jenkins, J. C. (2014). Updated generalized biomass equations for North American tree species. *Forestry*, *87*, 129–151.

Clark, D. B., & Clark, D. A. (1996). Abundance, growth and mortality of very large trees in Neotropical lowland rain forest. *Forest Ecology and Management*, *80*, 235–244.

Condit, R. (1998). Tropical forest census plots (p. 211). Berlin, Germany; Georgetown, TX: Springer-Verlag; R.G. Landes Company. [WorldCat]

Condit, R., Lao, S., Singh, A., Esufali, S., & Dolins, S. (2014). Data and database standards for permanent forest plots in a global network. *Forest Ecology and Management*, *316*, 21–31.

Coomes, D. A., Duncan, R. P., Allen, R. B., & Truscott, J. (2003). Disturbances prevent stem size-density distributions in natural forests from following scaling relationships. *Ecology Letters*, *6*, 980–989.

Das, A., Battles, J., Stephenson, N. L., & van Mantgem, P. J. (2011). The contribution of competition to tree mortality in old-growth coniferous forests. *Forest Ecology and Management*, *261*, 1203–1213.

Das, A. J., Larson, A. J., & Lutz, J. A. (2018). Individual species-area relationships in temperate coniferous forests. *Journal of Vegetation Science*, https://doi.org/10.1111/jvs.12611

Das, A. J., Stephenson, N. L., & Davis, K. P. (2016). Why do trees die? Characterizing the drivers of background tree mortality. *Ecology*, *97*, 2616–2627.

Enquist, B. J., Brown, J. H., & West, G. B. (1998). Allometric scaling of plant energetics and population density. *Nature*, *395*, 163–165.

Enquist, B. J., West, G. B., & Brown, J. H. (2009). Extensions and evaluations of a general quantitative theory of forest structure and dynamics. *Proceedings of the National Academy of Sciences USA*, *106*, 7046–7051.

Fauset, S., Johnson, M. O., Gloor, M., Baker, T. R., Monteagudo M, A., Brienen, R. J. W., … Phillips, O. L. (2015). Hyperdominance in Amazonia forest carbon cycling. *Nature Communications*, *6*, 6857.

Forest Resource Assessment. (2015). *Terms and definitions* (Working Paper 180). Rome, Italy: Food and Agriculture Organization of the United Nations. Retrieved from http://www.fao.org

Furniss, T. J., Larson, A. J., & Lutz, J. A. (2017). Reconciling niches and neutrality in a subalpine temperate forest. *Ecosphere*, *8*, e01847.

Gilbert, G. S., Howard, E., Ayala-Orozco, B., Bonilla-Moheno, M., Cummings, J., Langridge, S., … Swope, S. (2010). Beyond the tropics: Forest structure in a temperate forest mapped plot. *Journal of Vegetation Science*, *21*, 388–405.

Hixon, M. A., Johnson, D. W., & Sogard, S. M. (2014). BOFFFFs: On the importance of conserving old-growth structure in fishery populations. *ICES Journal of Marine Science*, *71*, 2171–2185.

Hubbell, S. P. (2001). *The unified neutral theory of biodiversity and biogeography* (p. 375). Princeton, NJ: Princeton University Press.

Keeton, W. S., & Franklin, J. F. (2005). Do remnant old-growth trees accelerate rates of succession in mature Douglas-fir forests? *Ecological Monographs*, *75*, 103–118.

Kenkel, N. C., & Orloci, L. (1986). Applying metric and nonmetric multidimensional scaling to ecological studies: Some new results. *Ecology*, *67*, 919–928.

Koch, G. W., Sillett, S. C., Jennings, G. M., & Davis, S. D. (2004). The limits to tree height. *Nature*, *428*, 851–854.

LaFrankie, J. V., Ashton, P. S., Chuyong, G. B., Co, L, Condit, R., Davies, S. J., … Villa, G. (2006). Contrasting structure and composition of the understory in species-rich tropical rain forests. *Ecology*, *87*, 2298–2305.

LaManna, J. A., Mangan, S. A., Alonso, A., Bourg, N. A., Brockelman, W. Y., Bunyavejchewin, S., … Myers, J. A. (2017). Negative density dependence contributes to global patterns of plant biodiversity. *Science*, *356*, 1389–1392.

Larson, A. J., & Franklin, J. F. (2010). The tree mortality regime in temperate old-growth coniferous forests: The role of physical damage. *Canadian Journal of Forest Research*, *40*, 2091–2103.

Lindenmayer, D. B., & Laurence, W. F. (2016). The ecology, distribution, conservation and management of large old trees. *Biological Reviews*, *92*, 1434–1458. https://doi.org/10.1111/brv.12290

Lindenmayer, D. B., Laurance, W. F., & Franklin, J. F. (2012). Global decline in large old trees. *Science*, *338*, 1305–1306.

Lindenmayer, D. B., Laurance, W. F., Franklin, J. F., Likens, G. E., Banks, S. C., Blanchard, W., … Stein, J. A. R. (2014). New policies for old trees: Averting a global crisis in a keystone ecological structure. *Conservation Letters*, *7*, 61–69.

Luo, Y., & Chen, H. Y. H. (2013). Observations from old forests underestimate climate change effects on tree mortality. *Nature Communications*, *4*, 1655.

Lutz, J. A. (2015). The evolution of long-term data for forestry: Large temperate research plots in an era of global change. *Northwest Science*, *89*, 255–269.

Lutz, J. A., Larson, A. J., Freund, J. A., Swanson, M. E., & Bible, K. J. (2013). The importance of large-diameter trees to forest structural heterogeneity. *PLoS One*, *8*, e82784.

Lutz, J. A., Larson, A. J., Furniss, T. J., Donato, D. C., Freund, J. A., Swanson, M. E., … Franklin, J. F. (2014). Spatially non-random tree mortality and ingrowth maintain equilibrium pattern in an old-growth *Pseudotsuga-Tsuga* forest. *Ecology*, *95*, 2047–2054.

Lutz, J. A., Larson, A. J., Swanson, M. E., & Freund, J. A. (2012). Ecological importance of large-diameter trees in a temperate mixed-conifer forest. *PLoS One*, *7*, e36131.

Lutz, J. A., Matchett, J. R., Tarnay, L. W., Smith, D. F., Becker, K. M. L., Furniss, T. J., & Brooks, M. L. (2017). Fire and the distribution and uncertainty of carbon sequestered as aboveground tree biomass in Yosemite and Sequoia & Kings Canyon National Parks. *Land*, *6*, 10–24.

Lutz, J. A., van Wagtendonk, J. W., & Franklin, J. F. (2009). Twentieth-century decline of large-diameter trees in Yosemite National Park, California, USA. *Forest Ecology and Management*, *257*, 2296–2307.

Martin, T. A., Brown, K. J., Kučera, J., Meinzer, F. C., Sprugel, D. G., & Hinckley, T. M. (2001). Control of transpiration in a 220-year old *Abies amabilis* forest. *Forest Ecology and Management*, *152*, 211–224.

Meakem, V., Tepley, A. J., Gonzalez-Akre, E. B., Herrmann, V., Muller-Landau, H. C., Wright, S. J., … Anderson-Teixeira, K. J. (2017). Role of tree size in moist tropical forest carbon cycling and water deficit response. *New Phytologist*, https://doi.org/10.1111/nph.14633

Memiaghe, H. R., Lutz, J. A., Korte, L., Alonso, A., & Kenfack, D. (2016). Ecological importance of small-diameter trees to the structure, diversity, and biomass of a tropical evergreen forest at Rabi, Gabon. *PLoS One*, *11*, e0154988.

Muller-Landau, H. C., Condit, R. S., Harms, K. E., Marks, C. O., Thomas, S. C., Bunyavejchewin, S., … Ashton, P. (2006). Comparing tropical forest tree size distributions with the predictions of metabolic ecology and equilibrium models. *Ecology Letters*, *9*, 589–602.

Musavi, T., Migliavacca, M., Reichstein, M., Kattge, J., Wirth, C., Black, T. A., … Mahecha, M. D. (2017). Stand age and species richness dampen interannual variation of ecosystem-level photosynthetic capacity. *Nature Ecology and Evolution*, *1*, 0048.

Needham, J., Merow, C., Butt, N., Malhi, Y., Marthews, T. R., Morecroft, M., & McMahon, S. M. (2016). Forest community response to invasive pathogens: The case of ash dieback in a British woodland. *Journal of Ecology*, *104*, 315–330.

Oksanen, J., Guillaume Blanchet, F., Friendly, M., Kindt, R., Legendre, P., McGlinn, D., ... Wagner, H. (2017). *vegan: Community ecology package* (R package version 2.44), https://CRAN.R-project.org/package=vegan

Oksanen, J., Kindt, R., & Simpson, G. L. (2016). *vegan3d: Static and dynamic 3D plots for the 'vegan' package* (R package version 1.0–1), https://CRAN.R-project.org/package=vegan3d

Ostertag, R., Inman-Narahari, F., Cordell, S., Giardina, C. P., & Sack, L. (2014). Forest structure in low-diversity tropical forests: A study of Hawaiian wet and dry forests. *PLoS One*, *9*, e103268.

Pan, Y., Birdsley, R. A., Phillips, O. L., & Jackson, R. B. (2013). The structure, distribution, and biomass of the world's forests. *Annual Review of Ecology, Evolution, and Systematics*, *44*, 593–622.

R Development Core Team. (2016). *R: A language and environment for statistical computing*. Vienna, Austria: R Foundation for Statistical Computing. Retrieved from http://www.R-project.org/

Rambo, T., & North, M. (2009). Canopy microclimate response to pattern and density of thinning in a Sierra Nevada forest. *Forest Ecology and Management*, *257*, 435–442.

Réjou-Méchain, M., Muller-Landau, H. C., Detto, M., Thomas, S. C., Le Toan, T., Saatchi, S. S., ... Chave, J. (2014). Local spatial structure of forest biomass and its consequences for remote sensing of carbon stocks. *Biogeosciences*, *11*, 6827–6840.

Saez, E., & Zucman, G. (2016). Wealth inequality in the United States since 1913: Evidence from capitalized income tax data. *The Quarterly Journal of Economics*, *131*, 519–578.

Sillett, S. C., Van Pelt, R., Kramer, R. D., Carroll, A. L., & Koch, G. W. (2015). Biomass and growth potential of *Eucalyptus regnans* up to 100 m tall. *Forest Ecology and Management*, *348*, 78–91.

Slik, J. W. F., Paoli, G., McGuire, K., Amaral, I., Barroso, J., Bastian, M., ... Zweifel, N. (2013). Large trees drive forest aboveground biomass variation in moist lowland forests across the tropics. *Global Ecology and Biogeography*, *22*, 1261–1271.

Spies, T. A., & Franklin, J. F. (1991). The structure of natural young, mature and old-growth Douglas-fir forests in Oregon and Washington. In L. F. Ruggiero, K. B. Aubry, A. B. Carey, & M. H. Huff (Eds.), *Wildlife and management of unmanaged Douglas-fir forests PNW-GTR-285* (pp. 91–109). Portland, OR: USDA Forest Service.

Stephenson, N. L., Das, A. J., Condit, R., Russo, S. E., Baker, P. J., Beckman, N. G., ... Zavala, M. A. (2014). Rate of tree carbon accumulation increases continuously with tree size. *Nature*, *507*, 90–93.

van Mantgem, P. J., Stephenson, N. L., Byrne, J. C., Daniels, L. D., Franklin, J. F., Fule, P. Z., ... Veblen, T. T. (2009). Widespread increase of tree mortality rates in the western United States. *Science*, *323*, 521–524.

Van Pelt, R., Sillett, S. C., Kruse, W. A., Freund, J. A., & Kramer, R. D. (2016). Emergent crowns and light-use complementarity lead to global maximum biomass and leaf area in *Sequoia sempervirens* forests. *Forest Ecology and Management*, *375*, 279–308.

van Wagtendonk, J. W., & Moore, P. E. (2010). Fuel deposition rates of montane and subalpine conifers in the central Sierra Nevada, California, USA. *Forest Ecology and Management*, *259*, 2122–2132.

Wang, C. (2006). Biomass allometric equations for 10 co-occurring tree species in Chinese temperate forests. *Forest Ecology and Management*, *222*, 9–16.

West, G. B., Brown, J. H., & Enquist, B. J. (1997). A general model for the origin of allometric scaling laws in biology. *Science*, *276*, 122–126.

West, G. B., Enquist, B. J., & Brown, J. H. (2009). A general quantitative theory of forest structure and dynamics. *Proceedings of the National Academy of Sciences USA*, *106*, 7040–7045.

Zanne, A. E., Lopez-Gonzalez, G., Coomes, D. A., Ilic, J., Jansen, S., Lewis, S. L., ... Chave, J. (2009). *Global wood density database*. Retrieved from https://doi.org/10.5061/dryad.234

BIOSKETCHES

James A. Lutz is an Assistant Professor of Forest Ecology at Utah State University. He studies forest ecosystems to contribute to science-based conservation and management with particular emphasis on demography and spatial patterns of tree mortality and the effects of fire on old-growth forest communities.

Tucker J. Furniss is a Ph.D. student at Utah State University. He studies spatial patterns of trees and demographic processes.

The ForestGEO Network includes the senior investigators who collaborated on this research. The Smithsonian ForestGEO network conducts long-term, large-scale research on forests around the world. This collaborative effort seeks to increase scientific understanding of forest ecosystems, guide sustainable forest management and natural-resource policies, monitor the impacts of global change and build capacity in forest science.

SUPPORTING INFORMATION

Additional Supporting Information may be found online in the supporting information tab for this article.

How to cite this article: Lutz JA, Furniss TJ, Johnson DJ, et al. Global importance of large-diameter trees. *Global Ecol Biogeogr*. 2018;00:1–16. https://doi.org/10.1111/geb.12747

APPENDIX

DATA REFERENCES

Allen, D., Vandermeer, J., & Perfecto, I. (2009). When are habitat patches really islands? *Forest Ecology and Management*, *258*, 2033–2036.

Arias Garcia, J. C., Duque, A., & Cárdenas, D. (2009). Crecimiento Diamétrico de un bosque del nor occidente Amazónico. *Revista Colombia Amazónica*, *2*, 57–64.

Bourg, N. A., McShea, W. J., Thompson, J. R., McGarvey, J. C., & Shen, X. (2013). Initial census, woody seedling, seed rain, and stand structure data for the SCBI SIGEO large forest dynamics plot. *Ecology*, *94*, 2111–2112.

Bunyavejchewin, S., Baker, P. J., LaFrankie, J. V., & Ashton, P. S. (2001). Stand structure of a seasonal dry evergreen forest at Huai Kha Khaeng Wildlife Sanctuary, western Thailand. *Natural History Bulletin of the Siam Society*, *49*, 89–106.

Butt, N., Campbell, G., Malhi, Y., Morecroft, M., Fenn, K., & Thomas, M. (2009). *Initial results from establishment of a long-term broadleaf monitoring plot at Wytham Woods*. Oxford, UK: University of Oxford Report.

Cao, M., Zhu, H., Wang, H., Lan, G., Hu, Y., Zhou, S., ... Cui, J. (2008). *Xishuangbanna tropical seasonal rainforest dynamics plot: Tree distribution maps, diameter tables and species documentation* (p. 266). Kunming, China: Yunnan Science and Technology Press.

Chao, W.-C., Song, G.-Z. M., Chao, K.-J., Liao, C.-C., Fan, S.-W., Wu, S.-H., ... Hsieh, C.-F. (2010). Lowland rainforests in southern Taiwan and Lanyu, at the northern border of paleotropics and under the influence of monsoon wind. *Plant Ecology*, *210*, 1–17.

Chen, L., Mi, X., Comita, L. S., Zhang, L., Ren, H., & Ma, K. (2010). Community-level consequences of density dependence and habitat association in a subtropical broad-leaved forest. *Ecology Letters*, *13*, 695–704.

Co, L., Lagunzad, D. A. LaFrankie, J. V. Bartolome, N. A., Molina, J. E., Yap, S. I., ... Davies, S. J. (2004). Palanan forest dynamics plot, Philippines. In E. Losos & E. Leigh (Eds.), *Tropical forest diversity and dynamism: Findings from a large-scale plot network* (pp. 574–584). IL: University of Chicago Press.

Condit, R., Aguilar, S., Hernandez, A., Perez, R., Lao, S., Angehr, G., ... Foster, R. B. (2004). Tropical forest dynamics across a rainfall gradient and the impact of an El Nino dry season. *Journal of Tropical Ecology*, *20*, 51–72.

de Oliveira, A. A., Vicentini, A., Chave, J., Castanho, C. D T., Davies, S. J., Martini, A. M. Z., ... Souza, V. C. (2014). Habitat specialization and phylogenetic structure of tree species in a coastal Brazilian white-sand forest. *Journal of Plant Ecology*, *7*, 134–144.

Georgiadis, N. J. (2011). Conserving wildlife in African landscapes: Kenya's Ewaso ecosystem. *Smithsonian Contributions to Zoology*, *632*, 1–123.

Gomes, A. C. S., Andrade, A., Barreto-Silva, J. S., Brenes-Arguedas, T., López, D. C., de Freitas, C. C., ... Vicentini, A. (2013). Local plant species delimitation in a highly diverse Amazonian forest: Do we all see the same species? *Journal of Vegetation Science*, *24*, 70–79.

Hubbell, S. P., Foster, R. B., O'Brien, S. T., Harms, K. E., Condit, R., Wechsler, B., ... de Lao, S. L. (1999). Light gap disturbances, recruitment limitation, and tree diversity in a neotropical forest. *Science*, *283*, 554–557.

Janík, D., Král, K., Adam, D., Hort, L., Samonil, P., Unar, P., ... McMahon, S. (2016). Tree spatial patterns of *Fagus sylvatica* expansion over 37 years. *Forest Ecology and Management*, *375*, 134–145.

Johnson, D. J., Bourg, N. A., Howe, R., McShea, W. J., Wolf, A., & Clay, K. (2014). Conspecific negative density-dependent mortality and the structure of temperate forests. *Ecology*, *95*, 2493–2503.

Kenfack, D., Thomas, D. W., Chuyong, G. B., & Condit, R. (2007). Rarity and abundance in a diverse African forest. *Biodiversity Conservation*, *16*, 2045–2074.

LaFrankie, J. V., Davies, S. J., Wang, L. K., Lee, S. K., & Lum, S. K. Y. (2005). *Forest trees of Bukit Timah: Population ecology in a tropical forest fragment* (p. 178). Singapore: Simply Green.

LaManna, J. A., Walton, M. L., Turner, B. L., & Myers, J. A. (2016). Negative density dependence is stronger in resource-rich environments and diversifies communities when stronger for common but not rare species. *Ecology Letters*, *19*, 657–667.

Lee, H. S., Ashton, P. S., Yamakura, T., Tan, S., Davies, S. J., Itoh, A., ... LaFrankie, J. V. (2005). *The 52-hectare forest research plot at Lambir Hills, Sarawak, Malaysia: Tree distribution maps, diameter tables and species documentation*. Kuching, Malaysia: Forest Department Sarawak, The Arnold Arboretum-CTFS Asia Program, Smithsonian Tropical Research Institute.

Lin, Y.-C., Chang, L.-W., Yang, K.-C., Wang, H.-H., & Sun, I. F. (2011). Point patterns of tree distribution determined by habitat heterogeneity and dispersal limitation. *Oecologia*, *165*, 175–184.

Makana, J., Hart, T. B., Liengola, I., Ewango, C., Hart, J. A., & Condit, R. (2004). Ituri forest dynamics plot, democratic Republic of Congo. In E. Losos & E. Leigh (Eds.), *Tropical forest diversity and dynamism: Findings from a large-scale plot network* (pp. 492–505). IL: University of Chicago Press.

Manokaran, N., Quah, E. S., AShton, P. S., LaFrankie, J. V., Noor, N. S. M., Ahmad, W. M. S. W., & Okuda, T (2004). Pasoh forest dynamics plot, Malaysia. In E. Losos & E. Leigh (Eds.), *Tropical forest diversity and dynamism: Findings from a large-scale plot network* (pp. 585–598). IL: University of Chicago Press.

McMahon, S. M., & Parker, G. G. (2014). A general model of intra-annual tree growth using dendrometer bands. *Ecology and Evolution*, *5*, 243–254.

Orwig, D. A., Foster, D. R., & Ellison, A. M. (2015). *Harvard forest CTFS-ForestGEO mapped forest plot since 2014*. Harvard Forest Data Archive: HF253. Retrieved from http://harvardforest.fas.harvard.edu:8080/exist/apps/datasets/showData.html?id=hf253

Su, S. H., Hsieh, C. F., Chang-Yang, C. H., Lu, C. L., & Guan, B. T. (2010). Micro-topographic differentiation of the tree species composition in a subtropical submontane rainforest in northeastern Taiwan. *Taiwan Journal of Forest Science*, *25*, 63–80.

Sukumar, R., Sathyanarayana, S., Dattaraja, H., John, R., & Joshi, N. (2004). Mudumalai forest dynamics plot, India. In E. Losos & E. Leigh (Eds.), *Tropical forest diversity and dynamism: Findings from a large-scale plot network* (pp. 551–563). IL: University of Chicago Press.

Valencia, R., Condit, R., Foster, R. B., Romoleroux, K., Munoz, G. V., Svenning, J.-C., ... Leigh, E. G. J. (2004). Yasuni forest dynamics plot, Ecuador. In E. Losos & E. Leigh (Eds.), *Tropical forest diversity and dynamism: Findings from a large-scale plot network* (pp. 609–620). IL: University of Chicago Press.

Vallejo, M., Samper, C., Mendoza, H., & Otero, J. (2004). La Planada forest dynamics plot, Colombia. In E. Losos & E. Leigh (Eds.), *Tropical forest diversity and dynamism: Findings from a large-scale plot network* (pp. 517–526). IL: University of Chicago Press.

Vincent, J. B., Henning, B., Saulei, S., Sosanika, G., & Weiblen, G. D. (2014). Forest carbon in lowland Papua New Guinea: Local variation and the importance of small trees. *Austral Ecology*, *40*, 151–159.

Wang, X., Wiegand, T., Wolf, A., Howe, R., Davies, S. J., & Hao, Z. (2011). Spatial patterns of tree species richness in two temperate forests. *Journal of Ecology*, *99*, 1382–1393.

Wu, S.-H., Hseu, Z. Y., Shih, Y. T., Sun, I. F., Wang, H. H., & Sen, Y. C. (2011). *Kenting Karst forest dynamics plot: Tree species characteristics and distribution patterns* (p. 306). Taipei, Taiwan: Taiwan Forestry Research Institute.

Xu, H., Li, Y., Lin, M., Wu, J., Luo, T., Zhou, Z., ... Liu, S. (2015). Community characteristics of a 60 ha dynamics plot in the tropical montane rain forest in Jianfengling, Hainan Island. *Biodiversity Science*, *23*, 192–201.

Yin, D., & He, F. (2014). A simple method for estimating species abundance from occurrence maps. *Methods in Ecology and Evolution*, *5*, 336–343.

Yuan, Z., Wang, S., Gazol, A., Mellard, J., Lin, F., Ye, J., ... Loreau, M. (2016). Multiple metrics of diversity have different effects on temperate forest functioning over succession. *Oecologia*, *182*, 1175–1185.

Zimmerman, J. K., Comita, L. S., Thompson, J., Uriarte, M., & Brokaw, N. (2010). Patch dynamics and community metastability of a subtropical forest: Compound effects of natural disturbance and human land use. *Landscape Ecology*, *25*, 1099–1111.

S1. Supplemental figures

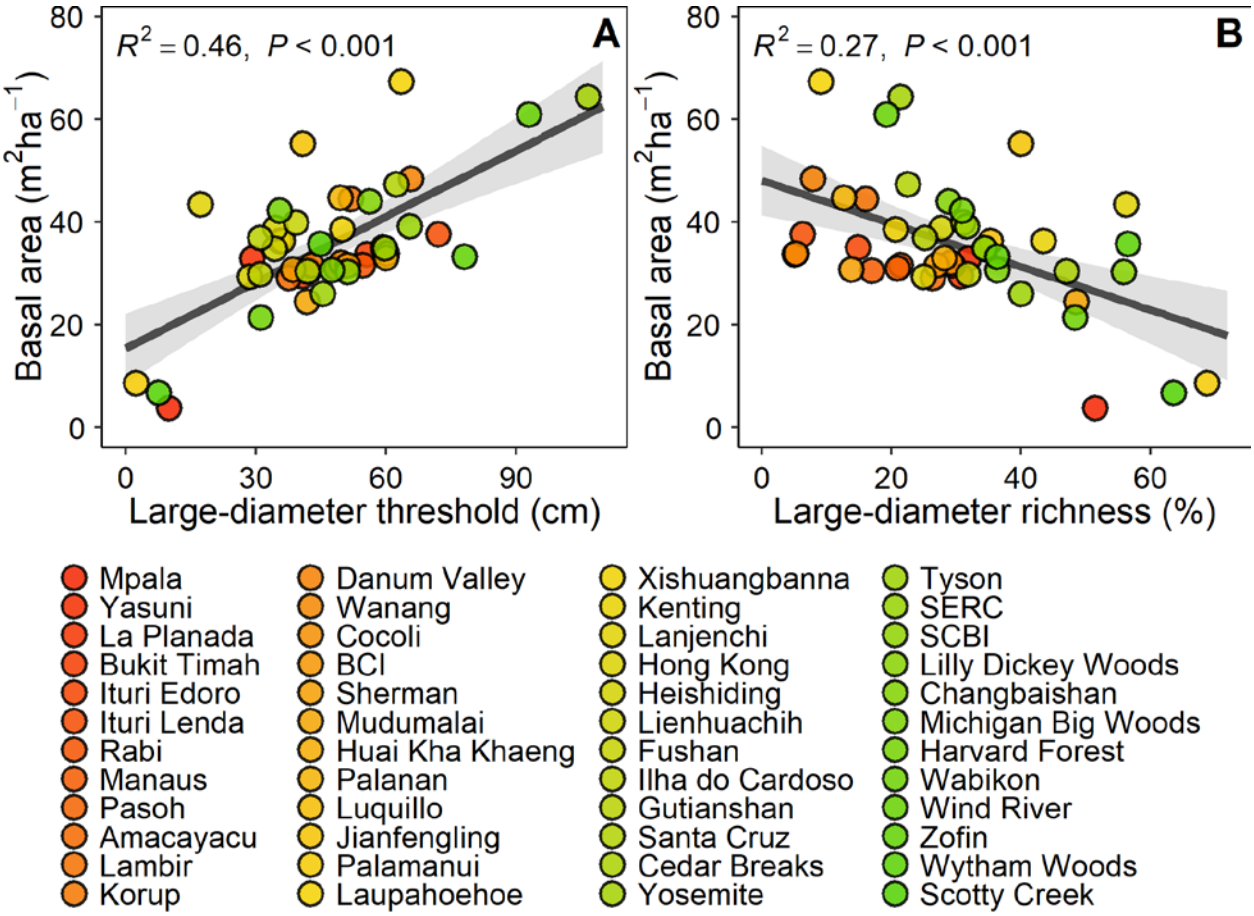

Fig. S1.1. The relationships among basal area and large-diameter threshold and large-diameter richness in 48 Smithsonian ForestGEO plots. This is corollary with Fig. 2, panels A and D, which show biomass instead of basal area. Colours indicate increasing absolute latitude from red to green.

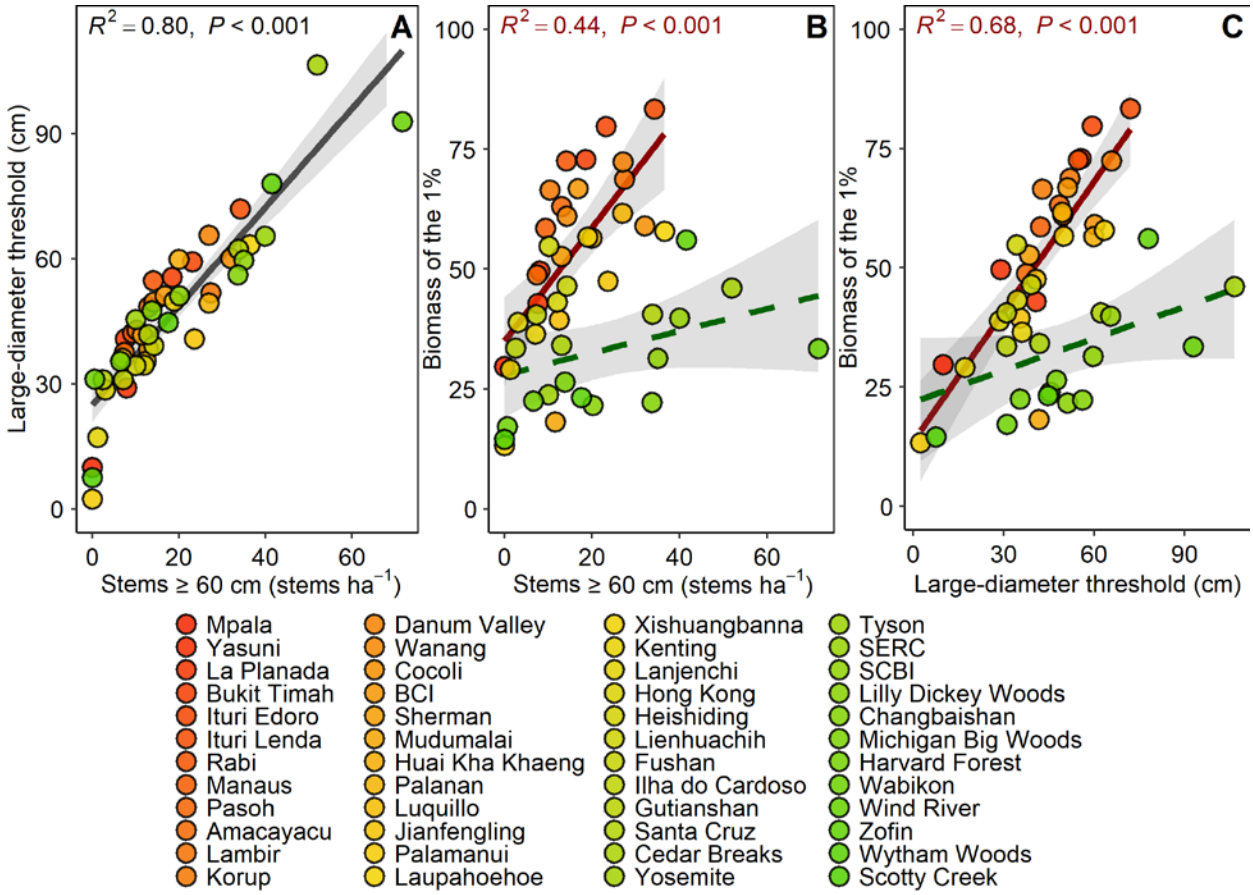

Fig. S1.2. The relationships among the metrics for the abundance of large-diameter trees. The relationship between stems ≥60 cm DBH and the large-diameter threshold was globally applicable (A), even including those plots with no stems ≥60 cm DBH. The relationship between stems and the biomass of the 1% or largest trees was not globally applicable (B), but there was a relationship for tropical plots (absolute latitude ≤23.5°), but not for temperate plots (P>0.05). Similarly, the relationship between the large-diameter threshold and the biomass of the 1% of largest trees was not globally applicable (C), although a relationship existed for tropical plots. Colours indicate increasing absolute latitude from red to green.

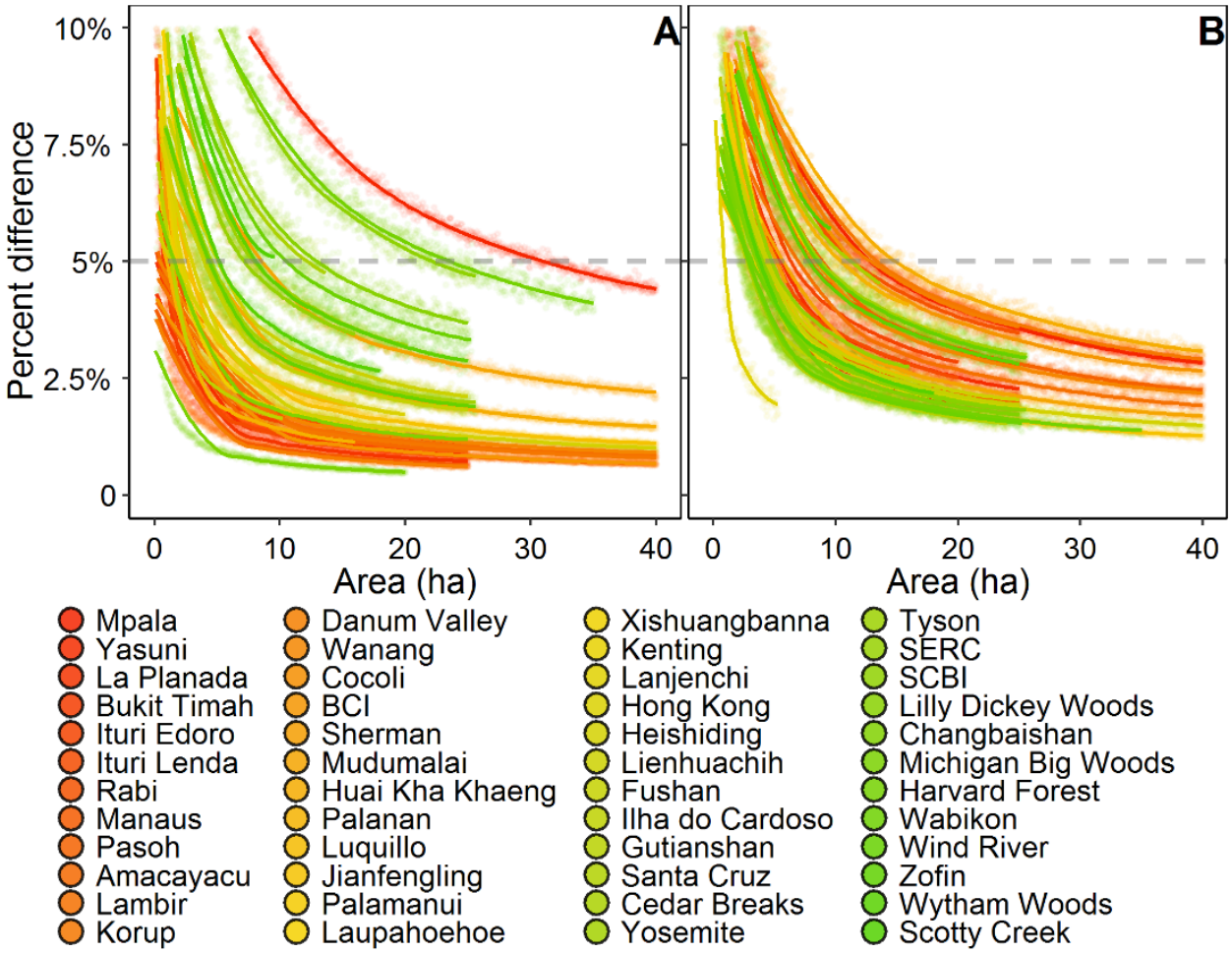

Fig. S1.3. Area needed to estimate biomass (A) and stem density (B) in 48 Smithsonian ForestGEO plots. Each point represents the percent deviation from the mean of a sample size equal to the number of 400 m^2 quadrats in each plot. Colours indicate increasing absolute latitude from red to green.

S3. Supplemental tables

Table S3.1. Characteristics of plots within the Smithsonian ForestGEO network. Stems indicates the number of woody stems ≥1 cm dbh within each plot. *E* represents the latitude derived coefficient for biomass calculation for tropical plots (absolute latitude ≤23.5°) from Chave *et al.* (2014), and extracted from http://chave.ups-tlse.fr/pantropical_allometry.htm#E on 12 December 2017.

Plot	Region	Latitude (°)	Longitude (°)	Area (ha)	Stems	*E*	Citation
Amacayacu	Tropical Latin America	-3.81	-70.27	25	123,696	-0.0792	Arias-Garcia *et al.* 2009
Barro Colorado Island	Tropical Latin America	9.15	-79.85	50	246,903	0.051764	Hubbell *et al.* 1999
Bukit Timah	Tropical Asia	1.35	103.78	2	12,546	-0.0848	LaFrankie *et al.* 2005
Cedar Breaks	Cold temperate / boreal	37.66	-112.85	13.64	23,238	–	Furniss *et al.* 2017
Changbaishan	Cold temperate / boreal	42.38	128.08	25	30,743	–	Yuan *et al.* 2016
Cocoli	Tropical Latin America	8.99	-79.62	4	8,654	0.070899	Condit *et al.* 2004
Danum Valley	Tropical Asia	5.1	117.69	25	189,316	-0.04479	–
Fushan	Temperate	24.76	121.56	25	111,958	–	Su *et al.* 2010
Gutianshan	Temperate	29.25	118.12	24	139,991	–	Chen *et al.* 2010
Harvard Forest	Cold temperate / boreal	42.54	-72.18	35	108,632	–	Orwig *et al.* 2015
Heishiding	Temperate	23.27	111.53	50	263,835	0.746412	Yin & He 2014
Hong Kong	Temperate	22.43	114.18	20	117,203	0.490652	–
Huai Kha Khaeng	Tropical Asia	15.63	99.22	50	125,296	0.319166	Bunyavejchewin *et al.* 2001
Ilha do Cardoso	Temperate	-25.1	-47.96	10.24	47,526	–	Oliveira *et al.* 2014
Ituri Edoro	Tropical Africa	1.44	28.58	20	179,120	0.003712	Makana *et al.* 2004
Ituri Lenda	Tropical Africa	1.44	28.58	20	151,068	0.003712	Makana *et al.* 2004
Jianfengling	Tropical Asia	18.73	108.90	60	391,628	0.280216	Xu *et al.* 2015
Kenting	Tropical Asia	21.98	120.8	9.6	36,201	0.099318	Wu *et al.* 2011
Korup	Tropical Africa	5.07	8.85	50	364,175	-0.08991	Kenfack *et al.* 2007
La Planada	Tropical Latin America	1.16	-77.99	25	100,746	-0.14564	Vallejo *et al.* 2004
Lambir	Tropical Asia	4.19	114.02	52	399,234	-0.1053	Lee *et al.* 2005
Lanjenchi	Tropical Asia	22.06	120.85	5.28	66,671	0.010925	Chao *et al.* 2010
Laupahoehoe	Tropical Oceania	19.93	-155.29	4	15,701	0.242613	Ostertag *et al.* 2014
Lienhuachih	Temperate	23.91	120.88	25	203,313	0.225027	Lin *et al.* 2011
Lilly Dickey Woods	Temperate	39.24	-86.22	25	27,824	–	Johnson *et al.* 2014
Luquillo	Tropical Latin America	18.33	-65.82	16	46,360	0.08761	Zimmerman *et al.* 2010
Manaus	Tropical Latin America	-2.44	-59.79	25	155,908	-0.11682	Gomes *et al.* 2013
Michigan Big Woods	Cold temperate / boreal	42.47	-84	20	45,564	–	Allen *et al.* 2009
Mpala	Tropical Africa	0.29	36.88	120	355,611	0.539807	Georgiadis *et al.* 2011
Mudumalai	Tropical Asia	11.6	76.53	50	30,402	0.209588	Sukumar *et al.* 2004
Palamanui	Tropical Oceania	19.74	-155.99	4	32,818	0.242613	Ostertag *et al.* 2014
Palanan	Tropical Asia	17.04	122.39	16	79,707	-0.02103	Co *et al.* 2004
Pasoh	Tropical Asia	2.98	102.31	50	286,769	-0.09398	Manokaran *et al.* 2004
Rabi	Tropical Africa	-1.92	9.88	25	199,703	0.012459	Memiaghe *et al.* 2016
Santa Cruz	Temperate	37.01	-122.08	6	11,708	–	Gilbert *et al.* 2010
SCBI	Temperate	38.89	-78.15	25.6	45,351	–	Bourg *et al.* 2013
Scotty Creek	Cold temperate / boreal	61.3	-121.3	9.6	40,391	–	Baltzer *et al.* 2014
SERC	Temperate	38.89	-76.56	16	33,379	–	McMahon & Parker 2014
Sherman	Tropical Latin America	9.28	-79.97	5.96	21,911	-0.04617	Condit *et al.* 2004
Tyson	Temperate	38.52	-90.56	20.16	30,283	–	LaManna *et al.* 2016
Wabikon	Cold temperate / boreal	45.55	-88.79	25.2	41,772	–	Wang *et al.* 2011
Wanang	Tropical Oceania	-5.25	145.27	50	276,139	-0.17639	Vincent *et al.* 2014
Wind River	Temperate	45.82	-121.96	25.6	31,005	–	Lutz *et al.* 2013
Wytham Woods	Temperate	51.77	-1.34	18	18,279	–	Butt *et al.* 2009
Xishuangbanna	Temperate	21.61	101.57	20	91,299	0.336188	Cao *et al.* 2008
Yasuni	Tropical Latin America	-0.69	-76.4	25	145,859	-0.02603	Valencia *et al.* 2004
Yosemite	Temperate	37.77	-119.82	25.6	35,925	–	Lutz *et al.* 2012
Žofín	Temperate	48.66	14.71	25	60,112	–	Janík *et al.* 2016
Total	48			1,278	5,601,473		

Table S3.2. Structural characteristics of stem density for global forests. Values for density (stems ha^{-1}) are shown for each diameter class, with mean and standard deviation (SD) given for each 100 m × 100 m of each plot.

	Diameter class (cm)													
	1 ≤ DBH < 5		5 ≤ DBH < 10		10 ≤ DBH < 30		30 ≤ DBH < 60		60 ≤ DBH < 90		DBH ≥ 90		All stems	
PLOT	Mean	(SD)	Mean	(SD)	Mean	(SD)	Mean	(SD)	Mean	(SD)	Mean	(SD)	Mean	(SD)
Amacayacu	3667	(457)	703	(68)	492	(36)	80	(12)	7	(3)	0	(1)	4948	(518)
Barro Colorado Island	3794	(422)	702	(91)	361	(46)	64	(9)	12	(4)	4	(2)	4938	(463)
Bukit Timah	5210	(265)	642	(55)	330	(44)	73	(4)	10	(4)	9	(6)	6273	(180)
Cedar Breaks	753	(537)	298	(204)	378	(216)	100	(53)	11	(9)	2	(2)	1542	(961)
Changbaishan	659	(148)	173	(43)	214	(31)	149	(15)	32	(8)	2	(1)	1230	(188)
Cocoli	1633	(242)	260	(19)	190	(16)	48	(9)	20	(5)	12	(3)	2164	(248)
Danum Valley	5853	(395)	1078	(80)	532	(45)	83	(13)	15	(6)	12	(6)	7573	(526)
Fushan	2975	(768)	694	(242)	696	(241)	100	(15)	12	(5)	3	(3)	4478	(1139)
Gutianshan	4344	(1439)	731	(183)	626	(72)	130	(29)	2	(2)	0	0	5833	(1580)
Harvard Forest	2011	(2706)	334	(192)	573	(226)	179	(57)	6	(10)	0	0	3104	(2600)
Heishiding	3748	(643)	771	(172)	638	(168)	107	(22)	11	(6)	1	(1)	5277	(706)
Hong Kong	4618	(939)	547	(141)	608	(153)	83	(24)	3	(2)	0	(1)	5860	(1056)
Huai Kha Khaeng	1705	(619)	341	(70)	374	(48)	65	(17)	14	(6)	6	(3)	2506	(674)
Ilha do Cardoso	3121	(485)	914	(107)	543	(75)	75	(9)	7	(5)	0	0	4660	(578)
Ituri Edoro	7588	(1244)	885	(89)	399	(34)	61	(10)	18	(5)	5	(3)	8956	(1270)
Ituri Lenda	6630	(804)	569	(72)	259	(55)	61	(19)	26	(7)	9	(4)	7553	(829)
Jianfengling	4866	(822)	766	(144)	701	(94)	169	(21)	20	(5)	3	(2)	6526	(993)
Kenting	2034	(262)	823	(125)	807	(82)	88	(17)	5	(4)	2	(1)	3760	(410)
Korup	5923	(856)	863	(156)	413	(44)	74	(14)	7	(3)	3	(3)	7283	(920)
La Planada	2544	(189)	886	(93)	514	(41)	78	(9)	7	(3)	0	(1)	4030	(243)
Lambir	6106	(1118)	875	(120)	535	(72)	90	(21)	21	(8)	7	(3)	7635	(1233)
Lanjenchi	8971	(2078)	1919	(634)	1108	(150)	76	(31)	1	0	0	0	12075	(2795)
Laupahoehoe	2036	(702)	662	(140)	1065	(88)	126	(25)	28	(8)	8	(4)	3925	(859)
Lienhuachih	4668	(1512)	802	(223)	570	(95)	81	(21)	9	(4)	1	(1)	6131	(1760)
Lilly Dickey Woods	584	(436)	199	(66)	203	(30)	106	(27)	19	(7)	1	(1)	1112	(441)
Luquillo	1659	(550)	429	(83)	700	(62)	102	(26)	10	(4)	2	(1)	2903	(626)
Manaus	4908	(427)	768	(60)	470	(35)	79	(15)	8	(3)	1	(1)	6234	(441)
Michigan Big Woods	1185	(497)	395	(90)	272	(72)	115	(27)	14	(6)	0	0	1981	(515)
Mpala	2525	(2831)	353	(179)	85	(69)	1	(1)	0	0	0	0	2963	(2902)
Mudumalai	158	(154)	122	(98)	225	(76)	91	(18)	10	(6)	1	(1)	608	(210)
Palamanui	7589	(1200)	298	(64)	316	(60)	1	(2)	0	0	0	0	8204	(1084)
Palanan	3602	(429)	697	(83)	573	(42)	83	(14)	19	(8)	8	(5)	4981	(489)
Pasoh	4341	(584)	844	(89)	476	(42)	62	(10)	10	(3)	3	(2)	5735	(631)
Rabi	6844	(826)	663	(81)	399	(54)	67	(12)	10	(4)	4	(3)	7988	(926)
Santa Cruz	1238	(466)	246	(65)	293	(96)	133	(32)	25	(9)	8	(7)	1944	(593)
SCBI	1351	(1707)	182	(56)	191	(39)	90	(14)	32	(11)	3	(2)	1850	(1637)
Scotty Creek	3079	(1243)	921	(396)	136	(129)	0	0	0	0	0	0	4136	(1407)
SERC	1514	(813)	260	(42)	182	(34)	90	(18)	34	(7)	6	(4)	2086	(792)
Sherman	2484	(356)	606	(127)	482	(164)	77	(6)	11	(5)	2	(2)	3662	(550)
Tyson Research Center	1087	(803)	211	(40)	184	(42)	110	(24)	10	(4)	0	(1)	1601	(751)
Wabikon	1041	(674)	214	(229)	343	(195)	94	(28)	1	(1)	0	0	1692	(1017)
Wanang	4299	(460)	706	(67)	420	(47)	83	(15)	12	(5)	2	(1)	5523	(520)
Wind River	660	(180)	222	(78)	188	(54)	64	(16)	46	(10)	26	(13)	1207	(273)
Wytham Woods	93	(56)	384	(157)	405	(158)	116	(25)	15	(7)	2	(2)	1016	(309)
Xishuangbanna	3164	(527)	789	(128)	503	(53)	90	(25)	15	(6)	4	(3)	4565	(650)
Yasuni	4239	(621)	898	(74)	614	(38)	76	(11)	7	(3)	1	(1)	5834	(692)
Yosemite	539	(141)	328	(86)	389	(115)	91	(21)	27	(9)	25	(9)	1399	(266)
Žofín	1800	(724)	363	(282)	156	(76)	44	(17)	32	(10)	10	(5)	2404	(982)

Table S3.3. Structural characteristics of tree biomass (Mg ha^{-1}) for global forests. Values for biomass are shown for each diameter class, with mean and standard deviation (SD) given for each 100 m × 100 m of each plot.

	Diameter class (cm)															
	1 ≤ DBH < 5		5 ≤ DBH < 10		10 ≤ DBH < 30		30 ≤ DBH < 60		60 ≤ DBH < 90		DBH ≥ 90		All stems	
PLOT	Mean	(SD)	Mean	(SD)	Mean	(SD)	Mean	(SD)	Mean	(SD)	Mean	(SD)	Mean	(SD)
Amacayacu	5.0	(0.5)	13.7	(1.5)	86.1	(6.6)	117.8	(20.9)	40.1	(18.0)	5.1	(9.3)	267.7	(32.6)
Barro Colorado Island	4.5	(0.5)	12.0	(1.9)	47.2	(7.7)	76.0	(10.9)	51.1	(17.4)	66.7	(41.9)	257.5	(49.4)
Bukit Timah	6.3	(0.4)	11.6	(0.7)	58.4	(1.2)	107.2	(22.1)	44.4	(17.3)	135.4	(102.4)	363.3	(140.4)
Cedar Breaks	0.5	(0.4)	2.4	(1.6)	39.0	(23.2)	72.1	(33.2)	33.8	(28.9)	20.0	(23.0)	167.8	(53.3)
Changbaishan	0.4	(0.1)	1.4	(0.3)	22.5	(3.0)	144.8	(17.0)	96.9	(25.9)	21.6	(19.0)	287.6	(33.2)
Cocoli	1.9	(0.3)	4.1	(0.5)	32.4	(5.2)	50.3	(8.5)	74.5	(19.0)	118.0	(44.1)	281.3	(37.0)
Danum Valley	7.5	(0.5)	18.8	(1.5)	83.1	(7.4)	106.6	(19.0)	77.0	(29.6)	193.0	(112.3)	485.8	(152.4)
Fushan	2.7	(0.9)	8.0	(3.1)	69.9	(20.0)	79.7	(13.7)	37.5	(17.6)	25.8	(28.2)	223.6	(25.3)
Gutianshan	3.8	(1.3)	8.3	(2.0)	74.1	(10.4)	91.7	(23.2)	6.7	(6.4)	0.0	0.0	184.6	(26.6)
Harvard Forest	1.8	(1.4)	5.0	(3.0)	85.4	(27.6)	148.7	(53.2)	19.2	(29.5)	0.4	(2.1)	260.5	(65.8)
Heishiding	2.1	(0.3)	6.4	(1.6)	49.8	(11.9)	62.1	(15.9)	22.6	(12.7)	5.5	(7.4)	148.5	(26.5)
Hong Kong	2.8	(0.7)	6.0	(1.8)	66.1	(14.9)	58.0	(19.4)	7.2	(6.2)	1.9	(3.6)	142.0	(19.8)
Huai Kha Khaeng	1.3	(0.4)	4.5	(0.9)	50.3	(7.2)	68.8	(17.4)	51.2	(21.6)	82.3	(51.4)	258.4	(65.4)
Ilha do Cardoso	3.2	(0.4)	10.9	(1.2)	56.9	(8.6)	56.4	(9.6)	21.0	(16.3)	0.0	0.0	148.4	(17.1)
Ituri Edoro	8.0	(1.4)	16.1	(1.2)	56.3	(5.6)	104.9	(15.5)	115.1	(31.1)	75.0	(47.4)	375.3	(46.0)
Ituri Lenda	6.5	(0.5)	9.8	(1.5)	43.9	(8.6)	111.5	(31.2)	166.5	(50.6)	129.3	(64.4)	467.4	(61.7)
Jianfengling	4.0	(0.7)	9.6	(1.8)	94.9	(12.2)	170.7	(21.7)	80.6	(18.9)	32.5	(21.2)	392.2	(37.0)
Kenting	2.9	(0.5)	15.1	(2.0)	104.7	(12.9)	87.4	(16.4)	19.7	(16.3)	24.9	(15.1)	254.7	(38.0)
Korup	8.1	(1.3)	15.2	(2.3)	84.3	(7.0)	110.4	(24.2)	44.9	(21.1)	82.1	(81.8)	345.0	(87.9)
La Planada	4.4	(0.3)	18.4	(1.9)	88.2	(8.8)	115.3	(14.5)	36.0	(17.1)	7.8	(14.9)	270.1	(29.7)
Lambir	7.3	(1.1)	16.5	(2.5)	93.7	(14.9)	143.6	(39.4)	127.6	(46.6)	106.7	(43.3)	495.4	(99.3)
Lanjenchi	7.7	(2.6)	17.2	(6.0)	63.1	(5.4)	23.5	(8.8)	1.4	(0.5)	0.0	0.0	113.0	(7.1)
Laupahoehoe	2.3	(0.9)	8.8	(1.9)	32.9	(3.2)	63.6	(17.7)	76.3	(21.3)	56.7	(25.4)	240.6	(45.0)
Lienhuachih	3.9	(1.2)	9.3	(2.5)	56.1	(8.5)	64.4	(16.1)	27.7	(12.1)	8.5	(9.5)	169.9	(25.4)
Lilly Dickey Woods	0.8	(0.4)	2.9	(1.0)	27.7	(4.5)	113.6	(31.7)	60.8	(24.8)	8.3	(10.7)	214.0	(28.7)
Luquillo	1.8	(0.4)	6.6	(1.1)	79.3	(11.9)	123.9	(33.3)	46.4	(17.6)	25.5	(20.9)	283.5	(52.8)
Manaus	6.8	(0.5)	15.8	(1.0)	96.3	(9.4)	141.5	(32.7)	56.9	(21.3)	26.3	(47.4)	343.6	(53.9)
Michigan Big Woods	1.5	(0.6)	5.0	(1.1)	28.6	(6.1)	118.3	(26.7)	37.9	(17.0)	0.5	(1.8)	191.8	(24.8)
Mpala	2.2	(1.4)	4.6	(2.5)	6.0	(5.4)	0.4	(0.8)	0.0	0.0	0.0	0.0	13.2	(8.4)
Mudumalai	0.2	(0.2)	1.4	(0.8)	40.5	(15.5)	108.6	(26.8)	42.7	(23.7)	11.3	(12.3)	204.7	(33.2)
Palamanui	18.7	(2.9)	3.2	(0.8)	6.3	(1.9)	1.4	(2.3)	0.0	0.0	0.0	0.0	29.6	(4.7)
Palanan	4.9	(0.5)	10.4	(1.4)	90.4	(8.4)	101.7	(20.9)	85.1	(37.2)	121.6	(79.0)	414.0	(118.8)
Pasoh	7.0	(0.8)	15.8	(1.7)	82.3	(7.5)	98.6	(16.3)	60.9	(21.7)	59.4	(42.7)	324.0	(55.3)
Rabi	6.9	(0.7)	11.6	(1.5)	69.9	(10.6)	98.6	(16.3)	58.2	(24.6)	78.1	(63.6)	323.2	(73.7)
Santa Cruz	1.2	(0.4)	3.7	(1.1)	42.5	(12.5)	127.1	(30.9)	92.5	(36.9)	94.6	(86.7)	361.5	(102.0)
SCBI	1.2	(1.0)	2.7	(0.8)	25.6	(5.1)	102.6	(18.5)	103.7	(35.1)	23.1	(17.8)	258.9	(43.1)
Scotty Creek	4.3	(1.9)	10.9	(4.9)	6.8	(7.7)	0.0	0.0	0.0	0.0	0.0	0.0	22.0	(11.1)
SERC	1.6	(0.5)	3.6	(0.6)	24.4	(5.7)	97.1	(21.2)	119.5	(27.4)	53.3	(38.9)	299.5	(49.1)
Sherman	3.5	(0.4)	10.3	(2.1)	71.6	(22.9)	100.9	(25.2)	54.9	(23.6)	33.4	(24.3)	274.5	(40.8)
Tyson Research Center	1.2	(0.7)	3.1	(0.5)	26.4	(8.6)	112.5	(20.5)	31.1	(12.6)	1.3	(3.8)	175.6	(15.7)
Wabikon	0.9	(0.8)	2.6	(2.8)	46.9	(10.8)	59.2	(18.9)	1.5	(2.9)	0.0	0.0	111.1	(13.6)
Wanang	5.2	(0.5)	12.1	(1.2)	72.5	(9.3)	126.4	(27.7)	71.8	(30.1)	35.9	(32.7)	324.0	(61.3)
Wind River	0.5	(0.2)	1.7	(0.6)	17.2	(4.8)	62.3	(17.7)	171.0	(37.5)	279.5	(174.8)	532.0	(161.3)
Wytham Woods	0.4	(0.2)	7.5	(3.0)	72.1	(29.2)	133.4	(29.7)	65.6	(30.8)	30.5	(31.0)	309.5	(46.4)
Xishuangbanna	3.4	(0.6)	10.3	(1.6)	61.3	(9.9)	93.4	(26.4)	58.3	(27.7)	53.7	(44.4)	280.5	(80.9)
Yasuni	5.8	(0.7)	16.0	(1.1)	93.2	(7.0)	96.7	(19.8)	30.4	(16.6)	18.9	(19.3)	261.0	(47.9)
Yosemite	0.4	(0.1)	2.7	(0.7)	35.8	(11.1)	73.0	(15.8)	97.2	(32.2)	349.7	(126.0)	558.8	(129.9)
Žofín	1.5	(0.8)	3.4	(2.8)	13.7	(4.0)	41.3	(13.2)	113.8	(37.6)	74.2	(40.4)	247.9	(66.5)

S4. Supplemental information: Individual plot acknowledgements

Amacayacu: The 25-ha Long-Term Ecological Research Project of Amacayacu is a collaborative project of the Instituto Amazónico de Investigaciones Científicas Sinchi and the Universidad Nacional de Colombia Sede Medellín, in partnership with the Unidad de Manejo Especial de Parques Naturales Nacionales and the Center for Tropical Forest Science of the Smithsonian Tropical Research Institute (CTFS). The Amacayacu Forest Dynamics Plot is part of the Center for Tropical Forest Science, a global network of large-scale demographic tree plots. We acknowledge the Director and staff of the Amacayacu National Park for supporting and maintaining the project in this National Park.

Barro Colorado Island: The BCI forest dynamics research project was made possible by National Science Foundation grants to Stephen P. Hubbell: DEB-0640386, DEB-0425651, DEB-0346488, DEB-0129874, DEB-00753102, DEB-9909347, DEB-9615226, DEB-9615226, DEB-9405933, DEB-9221033, DEB-9100058, DEB-8906869, DEB-8605042, DEB-8206992, DEB-7922197, support from the Center for Tropical Forest Science, the Smithsonian Tropical Research Institute, the John D. and Catherine T. MacArthur Foundation, the Mellon Foundation, the Small World Institute Fund, numerous private individuals, and through the hard work of over 100 people from 10 countries over the past two decades. The plot project is part the Center for Tropical Forest Science, a global network of large-scale demographic tree plots.

Bukit Timah: The Bukit Timah Dynamics Plot has been funded mainly by National Institute of Education of Nanyang Technological University and the Smithsonian Tropical Research Institute.

Cedar Breaks: The Utah Forest Dynamics Plot is a collaborative project of Utah State University and the Utah Agricultural Experiment Station. We thank Cedar Breaks National Monument for providing logistical support, and the students, volunteers and staff individually listed at http://ufdp.org for data collection.

Changbaishan: Zhanqing Hao and Xugao Wang were supported by The National Key Research and Development Program of China (2016YFC0500302), National Natural Science Foundation of China (31570432 and 31370444), Key Research Program of Frontier Sciences, CAS (QYZDB-SSW-DQC002).

Danum Valley: The Danum plot is a core project of the Southeast Asia Rain Forest Research Partnership (SEARRP). We thank SEARRP partners especially Yayasan Sabah for their support, and HSBC Malaysia and the University of Zurich for funding. We are grateful to the research assistants who are conducting the census, in particular the team leader Alex Karolus, and to Mike Bernados and Bill McDonald for species identifications. We thank Stuart Davies and Shameema Esufali for advice and training.

Fushan: Taiwan Forestry Bureau, Taiwan Forestry Research Institute, National Taiwan University (Institute of Ecology and Evolutionary Biology), and the Center for Tropical Forest Science of the Smithsonian Tropical Research Institute.

Gutianshan: We thank Drs. Mingjian Yu from Zhejiang University, Jianhua Chen for their contributions to the establishment and census of the 24-ha permanent forest plot. We gratefully acknowledge support from the Administration Bureau of the Gutianshan National Nature Reserve.

Harvard Forest: Funding for the Harvard ForestGEO Forest Dynamics plot was provided by the Center for Tropical Forest Science and Smithsonian Institute's Forest Global Earth Observatory (CTFS-ForestGEO), the National Science Foundation's LTER program (DEB 06-20443 and DEB 12-37491) and Harvard University. Thanks to many field technicians who helped census the plot and Jason Aylward for field supervision, data screening and database management. Thanks to John Wisnewski and the woods crew for providing materials, supplies, and invaluable field assistance with plot logistics and to David Foster for his support and assistance with plot design, location, and integration with other long-term studies at HF.

Heishiding: We thank Sun Yat-sen University in Guangzhou, China for funding the Heishiding research forest plot.

Hong Kong: We thank HSBC for funding the plot and the Policy for Sustainability Lab, Faculty of Social Sciences, HKU for coordinating the project.

Huai Kha Khaeng: The Huai Kha Khaeng 50-hectare plot project has been financially and administratively supported by many institutions and agencies. Direct financial support for the plot has been provided by the Royal Thai Forest Department and the National Parks Wildlife and Plant Conservation Department, the Arnold Arboretum of Harvard University (under NSF award #DEB-0075334, and grants from USAID and the Rockefeller Foundation), the Smithsonian Tropical Research Institute, and the National Institute for Environmental Studies, Japan. The Huai Kha Khaeng Forest Dynamics Plot is part the Center for Tropical Forest Science, a global network of large-scale demographic tree plots. We acknowledge the Royal Thai Forest Department for supporting and maintaining the project in Huai Kha Khaeng Wildlife Sanctuary, Thailand.

Ituri: The Ituri 40-ha plot program is a collaborative project between the Centre de Formation et de Recherche en Conservation Forestière, the Wildlife Conservation Society – DRC through his conservation project in the Okapi Forest Reserve, in partnership with the Center for Tropical Forest Science of the Smithsonian Tropical Research Institute. The Ituri plots are financially supported by the Wildlife Conservation Society, the Frank Levinson Family Foundation, and the Smithsonian Forest Global Earth Observatory. The Institut Congolais pour la Conservation de la Nature graciously provided the research permit.

Jianfengling: This research was supported by the Central Public-interest Scientific Institution Basal Research Fund (CAFYBB2017ZE001).

Kenting: The 2008 tree census was funded by a grant to SHW from the Council of Agriculture grant, Taiwan.

Korup: The 50-ha Korup Forest Dynamics Plot is affiliated with the Smithsonian's Center for Tropical Forest Science - Forest Global Earth Observatory. The 3 principal investigators gratefully acknowledge funding and other support received from CTFS for our first and second

censuses. Funding from the Botanical Research Foundation of Idaho is also gratefully acknowledged. Permission to conduct the field program in Cameroon is provided by the Ministry of Environment and Forests and the Ministry of Scientific Research and Innovation. We also acknowledge the dedicated support of our field team, especially field leadership by Sainge Nsanyi Moses and botanical work by Ekole Mambo Peter.

Lambir: The 52-ha Long-Term Ecological Research Project is a collaborative project of the Forest Department of Sarawak, Malaysia, the Center for Tropical Forest Science of the Smithsonian Tropical Research Institute, the Arnold Arboretum of Harvard University, USA (under NSF awards DEB-9107247 and DEB-9629601), and Osaka City, Ehime & Kyoto Universities, Japan (under Monbusho/JSPS Kekenhi grants 06041094, 08NP0901, 09NP0901, 26304027, and 17H04602). The Lambir Forest Dynamics Plot is part the Center for Tropical Forest Science, a global network of large-scale demographic tree plots. We acknowledge the Sarawak Forest Department for supporting and maintaining the project in Lambir Hills National Park.

Lanjenchi: The Lanjenchi plot has been supported by the Taiwan Forestry Bureau, Kenting National Park, the National Science Council of Taiwan, and the Center for Tropical Forest Science of the Smithsonian tropical Research Institute.

Laupahoehoe and **Palamanui**: This work is possible because of support provided by NSF EPSCoR (Grant Numbers EPS- 0554657 and EPS-0903833), the USDA Forest Service, the University of Hawaii, and the University of California at Los Angeles. I/We thank the USDA Forest Service and State of Hawaii Department of Land and Natural Resources Division of Forestry and Wildlife for access to the Hawaii Experimental Tropical Forest. For Palamanui we acknowledge the Hunt Companies, especially Roger Harris, for access to this lowland dry forest site.

Lienhuachih: The Taiwan Forestry Research Institute, Taiwan Forestry Bureau, Taiwan Academy of Ecology, Tunghai University (Taiwan), and the Center for Tropical Forest Science of the Smithsonian Tropical Research Institute.

Lilly Dickey Woods: Funding for the Lilly Dickey Woods Forest Dynamics Plot was provided by the Indiana Academy of Sciences, Indiana University Research and Teaching Preserve, and the Smithsonian Institution's Center for Tropical Forest Science.

Luquillo: This research was supported by grants BSR-8811902, DEB 9411973, DEB 0080538, DEB 0218039, DEB 0620910, DEB 0963447 AND DEB-129764 from NSF to the Department of Environmental Science, University of Puerto Rico, and to the International Institute of Tropical Forestry, USDA Forest Service, as part of the Luquillo Long-Term Ecological Research Program. The U.S. Forest Service (Dept. of Agriculture) and the University of Puerto Rico gave additional support. The LFDP is part of the Smithsonian Institution Forest Global Earth Observatory, a worldwide network of large, long-term forest dynamics plots.

Michigan Big Woods: We would like to thank the University of Michigan and Middlebury College students who have helped with all of the censuses of the Big Woods Plot. These censuses were supported by the Edwin S. George Reserve Fund, a USDA McIntyre-Stennis Grant, and the Middlebury College Millennium Fund.

Mpala: The 120-ha Mpala plot is a collaborative project of the National Museums of Kenya, the Kenya Wildlife Service, and the Mpala Wildlife Foundation, in partnership with the Center for Tropical Science Forest Global Earth Observatory of the Smithsonian Tropical Research Institute. Funding for the first census was provided by the Center for Tropical Forest Science – Forest Global Earth Observatory.

Mudumalai: Funding was received from the Ministry of Environment, Forest and Climate Change, Government of India and the Department of Biotechnology, Government of India. R Sukumar was a JC Bose National Fellow during the tenure of this work.

Palanan: Funding since 2010 had been provided by the Biodiversity Research Laboratory, Institute of Biology, University of the Philippines Diliman (BRL UP Biology), University of the Philippines Office of the Vice President for Academic Affairs under the Emerging Interdisciplinary Developing Research Program (EIDR), the University of the Philippines Diliman Office of the Vice Chancellor for Research and Development (UPD OVCRD), the Commission on Higher Education (CHED), the Department of Science and Technology-Philippine Council for Agriculture, Aquatic Resources Research and Development (DOST-PCAARRD), the Energy Development Corporation (EDC), the Forest Foundation Philippines, the Diliman Science Research Foundation and the Smithsonian Tropical Research Institute (STRI). Permits to work in the Northern Sierra Madre Natural Park were issued by its Protected Area Management Board (PAMB) through the cooperation of Biodiversity Management Bureau's Department of Environment and National Resource (BMB-DENR), Local Government of Palanan, Isabela. The plot was established by the Isabela State University (Philippines), Conservation International, PLAN, and the Arnold Arboretum of Harvard University (USA).

Rabi: The Rabi 25-ha is a collaborative project of the National Center for Scientific and Technical Research (CENAREST) in Gabon, the Center for Conservation and Sustainability (CCS) of the Smithsonian Conservation Biology Institute (SCBI) and the Center for Tropical Forest Science - Forest Global Earth Observatory (CTFS-ForestGEO) of the Smithsonian Tropical Research Institute. Funding for the first census was provided by Shell Gabon, CTFS-ForestGEO, and SCBI. Permission to conduct the field program in Gabon is provided by CENAREST. The plot is located in a conservation area of between a forest concession of the Compagnie des Bois du Gabon (CBG) and oil company Shell.

Santa Cruz: The UCSC Forest Ecology Research Plot was made possible by National Science Foundation grants to Gregory S. Gilbert (DEB-0515520 and DEB-084259), by the Pepper-Giberson Chair Fund, the University of California, the UCSC Campus Natural Reserve, and the hard work of dozens of UCSC students. The plot project is part the Center for Tropical Forest Science, a global network of large-scale demographic tree plots.

SCBI: Funding for the Smithsonian Conservation Biology Institute (SCBI) large forest dynamics plot was provided by the Smithsonian Institution (Forest Global Earth Observatory and the National Zoological Park, and the HSBC Climate Partnership.

Scotty Creek: The Scotty Creek plot establishment was supported by funds to JLB from the Canadian Foundation for Innovation, Ontario Ministry of Research and Innovation, and Canadian Foundation for Climate and Atmospheric Sciences. We are grateful to Rajit Patankar and Cory Wallace for their leadership in plot establishment and the hard work of many field assistants.

SERC: Smithsonian Environmental Research Center, Earthwatch Institute

Tyson: The Tyson Research Center Forest Dynamics Plot (TRCP) is supported by Washington University in St. Louis' Tyson Research Center. Funding was provided by the International Center for Advanced Renewable Energy and Sustainability (I-CARES) at Washington University in St. Louis, the National Science Foundation (DEB 1557094), and the Tyson Research Center. We thank the Tyson Research Center staff for providing logistical support, and the more than 100 high school students, undergraduate students, and researchers that have contributed to the project. The TRCP is part of the Center for Tropical Forest Science-Forest Global Earth Observatory (CTFS-ForestGEO), a global network of large-scale forest dynamics plots.

Wabikon: The Wabikon Lake Forest Dynamics Plot, located in the Chequamegon-Nicolet National Forest of northern Wisconsin, is part of the Smithsonian Institution's CTFS-ForestGEO network. Tree censuses at the site have been supported by the 1923 Fund, the Smithsonian Tropical Research Institute, and the Cofrin Center for Biodiversity at the University of Wisconsin-Green Bay. More than 50 scientists and student assistants contributed to the first two plot censuses. We are particularly grateful for the leadership of Gary Fewless, Steve Dhein, Kathryn Corio, Juniper Sundance, Cindy Burtley, Curt Rollman, Mike Stiefvater, Kim McKeefry, and U.S. Forest Service collaborators Linda Parker and Steve Janke.

Wanang: The 50-ha Wanang Forest Dynamics Plot is a collaborative project of the New Guinea Binatang Research Center, the Center for Tropical Forest Science of the Smithsonian Tropical Research Institute, the Forest Research Institute of Papua New Guinea, the Czech Academy of Sciences and the University of Minnesota supported by NSF DEB-0816749 and the Czech Science Foundation 16-18022S. We acknowledge the government of Papua New Guinea and the customary landowners of Wanang for supporting and maintaining the plot.

Wind River: The Wind River Forest Dynamics Plot is a collaborative project of Utah State University, the University of Montana, the University of Washington, and Washington State University. Funding was provided by the Center for Tropical Forest Science of the Smithsonian Tropical Research Institute, Utah State University, and the University of Washington. We acknowledge the Gifford Pinchot National Forest and the Wind River Field Station for providing logistical support, and the students, volunteers and staff individually listed at http://wfdp.org for data collection. The Wind River Forest Dynamics Plot was made possible by a grant from Jennifer Walston Johnson to the Smithsonian ForestGEO.

Wytham Woods: The 18-ha Long-Term Forest Monitoring Plot is a collaborative project between the University of Oxford, the Centre for Ecology and Hydrology, and the Smithsonian Institution CTFS – ForestGEO (HSBC Climate Partnership). The Wytham Forest Monitoring Plot is part of CTFS – ForestGEO, a global network of large-scale demographic tree plots.

Xishuangbanna: This research was supported by the National Science Foundation of China (31570380, 31300358), the Natural Science Foundation of Yunnan Province (2015FB185), the Southeast Asia Biodiversity Research Institute, Chinese Academy of Sciences (2016CASSEABRIQG002).

Yasuni: We gratefully acknowledge the professional help of numerous biologists and field collaborators of the Yasuni forest dynamics plot, particularly Álvaro Pérez, Pablo Alvia and Milton Zambrano, who provided invaluable expertise on plant taxonomy. Consuelo Hernández organized the data and improved its quality. Pontificia Universidad Católica del Ecuador (PUCE) and STRI co-financed the first two censuses of the plot. The third census was financed with funds of the Government of Ecuador and PUCE. Seed traps and seedling plots are monitored for over 10 years thanks to STRI and two awards from the NSF program LTREB (DBI 0614525 and 1122634). STRI also sponsored the Carbon Dynamics Initiative. This study was endorsed by the Ministerio de Ambiente del Ecuador permits MAE: No 004-2012-IC-FLO-MAE-DPO, 09-FLO-MA-DPO-PNY and 06-2011-FAU-DPAP.

Yosemite: The Yosemite Forest Dynamics Plot is a collaborative project of Utah State University, the University of Montana, and Washington State University. Funding was provided by the Center for Tropical Forest Science of the Smithsonian Tropical Research Institute, Utah State University, and the University of Washington. We thank Yosemite National Park for providing logistical support, and the students, volunteers and staff individually listed at http://yfdp.org for data collection. The Yosemite Forest Dynamics Plot was made possible by a grant from Jennifer Walston Johnson to the Smithsonian ForestGEO.

Žofín: The Žofín Forest Dynamics Plot is part of the Smithsonian Institution Forest Global Earth Observatory, a worldwide network of large, long-term forest dynamics plots. We acknowledge the Department of Forest Ecology of the Silva Tarouca Research Institute for supporting and maintaining the long-term monitoring of the Žofín Forest Dynamics Plot (under GA CR grant No. P504/15-23242S).